

1 **New tools for carbohydrate sulphation analysis: Heparan Sulphate 2-O-**
2 **sulphotransferase (HS2ST) is a target for small molecule protein kinase inhibitors**

3 Dominic P Byrne*, Yong Li*, Krithika Ramakrishnan*, Igor L Barsukov*, Edwin A Yates*, Claire E
4 Eyers*§, Dulcé Papy-Garcia†, Sandrine Chantepie†, Vijayakanth Pagadala#, Jian Liu+, Carrow
5 Wells^, David H Drewry^, William J Zuercher^¶, Neil G Berry‡, David G Fernig* and Patrick A
6 Eyers*||

7 * Department of Biochemistry, Institute of Integrative Biology, University of Liverpool, L69 7ZB,
8 UK.

9 § Centre for Proteome Research, Institute of Integrative Biology, University of Liverpool, L69 7ZB,
10 UK.

11 † Laboratory CRRET CNRS 9215, Université Paris-Est, CRRET (EA 4397/ERL CNRS 9215),
12 UPEC, F-94010, Créteil, France.

13 # Glycan Therapeutics, 617 Hutton Street, Raleigh, NC 27606, USA.

14 + UNC Eshelman School of Pharmacy, University of North Carolina at Chapel Hill, Chapel Hill, NC,
15 27599, USA.

16 ^ Structural Genomics Consortium, UNC Eshelman School of Pharmacy, University of North
17 Carolina at Chapel Hill, Chapel Hill, NC, 27599, USA.

18 ¶ Lineberger Comprehensive Cancer Center, University of North Carolina at Chapel Hill, Chapel Hill,
19 NC 27599, USA.

20 ‡ Department of Chemistry, University of Liverpool, L69 7ZD, UK

21 || Correspondence to Patrick.eyers@liverpool.ac.uk

22

23 **ABSTRACT:**

24 Sulphation of carbohydrate residues occurs on a variety of glycans destined for secretion, and this
25 modification is essential for efficient matrix-based signal transduction. Heparan sulphate (HS)
26 glycosaminoglycans control physiological functions ranging from blood coagulation to cell
27 proliferation. HS biosynthesis involves membrane-bound Golgi sulphotransferases, including heparan
28 sulphate 2-*O*-sulphotransferase (HS2ST), which transfers sulphate from the co-factor PAPS (3'-
29 phosphoadenosine 5'-phosphosulphate) to the 2-*O* position of α -L-iduronate in the maturing
30 oligosaccharide chain. The current lack of simple non-radioactive enzyme assays that can be used to
31 quantify the levels of carbohydrate sulphation hampers kinetic analysis of this process and the
32 discovery of HS2ST inhibitors. In this paper, we describe a new procedure for thermal shift analysis
33 of purified HS2ST. Using this approach, we quantify HS2ST-catalyzed oligosaccharide sulphation
34 using a novel synthetic fluorescent substrate and screen the Published Kinase Inhibitor Set (PKIS), to
35 evaluate compounds that inhibit catalysis. We report the susceptibility of HS2ST to a variety of cell
36 permeable compounds *in vitro*, including polyanionic polar molecules, the protein kinase inhibitor
37 rottlerin and oxindole-based RAF kinase inhibitors. In a related study, published back-to-back with
38 this article, we demonstrate that Tyrosyl Protein Sulpho Transferases (TPSTs) are also inhibited by a
39 variety of protein kinase inhibitors. We propose that appropriately validated small molecule
40 compounds could become new tools for rapid inhibition of glycan (and protein) sulphation in cells,
41 and that protein kinase inhibitors might be repurposed or redesigned for the specific inhibition
42 of HS2ST.

43 **SHORT TITLE:** Inhibition of HS2ST by protein kinase inhibitors

44 **ABBREVIATIONS:** **DSF:** Differential Scanning Fluorimetry; **GlcA:** β -D-glucouronate; **HS2ST:**
45 heparan sulphate 2-*O*-sulphotransferase **IdoA:** α -L-iduronate; **PAPS:** (Adenosine 3'-phosphate 5'-
46 phosphosulphate; **PKIS:** Published Kinase Inhibitor Set; **RAF:** Rapidly Accelerated Fibrosarcoma;
47 **TSA:** Thermostability Assay

48 **KEYWORDS:** HS2ST, PAPS, glycan, substrate PAPS, screening, enzyme, kinase, inhibitor

49 **SUMMARY STATEMENT:** We report that HS2ST, which is a PAPS-dependent glycan
50 sulphotransferase, can be assayed using a variety of novel biochemical procedures, including a non-
51 radioactive enzyme-based assay that detects glycan substrate sulphation in real time. HS2ST activity
52 can be inhibited by different classes of compounds, including known protein kinase inhibitors,
53 suggesting new approaches to evaluate the roles of HS2ST-dependent sulphation with small
54 molecules in cells.

55 **WORD COUNT INCLUDING REFERENCES: 10,595**

56 **INTRODUCTION:**

57 Biological sulphation is a widespread reversible covalent modification found throughout nature [1].
58 The regulated sulphation of saccharides is critical for cellular signalling, including regulatory
59 interactions between extracellular glycoproteins that control signal transduction and high-affinity
60 interactions between different cellular surfaces [2]. In addition to providing mechanical strength, the
61 sulphate-rich extracellular matrix also represents a hub for sulphation-based communication through
62 growth factor signalling [3]. For example, FGF-receptor interactions and intracellular signaling to the
63 ERK pathway are blunted in the absence of appropriate 2-*O* sulphation driven by Heparan Sulphate
64 (HS)-modifying enzymes [4-9], while sulphation of the tetrasaccharide Sialyl Lewis^x antigen on
65 glycolipids controls leukocyte adhesion to the endothelium during inflammation [10, 11].
66 Inappropriate glycan sulphation can therefore underlie aspects of abnormal signalling, infection,
67 inflammation and, increasingly, human neuropathies [12], suggesting that targeting of carbohydrate
68 sulphation dynamics using small molecule enzyme inhibitors remains a priority in both basic and
69 translational research [13]. Indeed, the current limited chemical toolbox to rapidly modify and study
70 glycan sulphation is based around small molecule inhibitors of Sulphatase-2 (Sulf-2), such as OKN-
71 007 [14] or heparanase inhibitors and HS mimics, including roneparstat and PG545, which have been
72 employed for basic and clinical investigation [15].

73 Glycan sulphotransferases (STs) can be classified into several families depending upon the positional
74 substrate specificity of enzymes for their respective sugar substrates [16, 17]. Heparan Sulphate 2-*O*-
75 sulphotransferase (HS2ST) is required for the generation of Heparan Sulphate (HS), which is an
76 abundant unbranched extracellular glycosaminoglycan with key roles in a range of physiological
77 functions, most notably growth-factor dependent signalling related to development, cell migration and
78 inflammation [18]. HS2ST is a transmembrane protein whose catalytic domain faces into the lumen of
79 the Golgi compartment, and catalyses the sulphation of iduronic acid and, to a lesser extent β -D-
80 glucouronate (GlcA), during the enzymatic assembly of secretory proteoglycans such as HS [18, 19].
81 HS2ST transfers the sulpho-moiety from PAPS (3'-phosphoadenosine 5'-phosphosulphate) sulphate
82 donor to the C2 hydroxyl of IdoA that lies adjacent to an *N*-sulphated glucosamine residue, generating
83 a 2-*O*-sulphated saccharide unit [20-22]. Removal of the sulphate by endosulphatases such as Sulf-2,
84 or more general HS processing by heparanase, also contributes to the complex physiological patterns
85 of carbohydrate editing found *in vivo* [23].

86 The analysis of murine models lacking HS2ST reveals central roles for 2-*O*-sulphated HS in kidney
87 development and neuronal function, and for signalling through Wnt and FGF-dependent pathways [8,
88 18, 24-26]. However, in order to carefully control and examine the dynamics and structural
89 heterogeneity of 2-*O* sulphation patterns in HS, which are the consequences of nontemplate-based
90 synthesis of HS and complex dynamic sulphation patterns, new small molecule approaches for the

91 direct, reversible, inhibition of sulphotransferase enzymes are urgently required. In particular, these
92 need to be deployed using chemical biology strategies to overcome deficiencies associated with
93 genetic disruption approaches relevant to development and/or compensatory glycosylation or
94 signalling mechanisms [27].

95 Mechanistic parallels between the enzymatic pathway of biological sulphation by sulphotransferases
96 [28] and phosphorylation by protein kinases [29] are apparent, since both enzyme classes transfer
97 charged chemical units from an adenine-based nucleotide co-factor to a (usually) polymeric acceptor
98 structure. The biological analysis of protein kinases, which are thought to employ a similar ‘in-line’
99 enzyme reaction as the 2-*O* sulphotransferases [28] when transferring phosphate to peptide targets
100 [30], has been revolutionised by the synthesis and wide availability of small molecule inhibitors [31].
101 Many of these compounds were originally discovered in screens with ATP-competitive inhibitor
102 libraries using oncology-associated target enzymes [32]. Protein kinases have proven to be
103 exceptional targets for the development of therapeutic agents in humans, and dozens of kinase
104 inhibitors have been approved, or will soon be approved, for cancer and anti-inflammatory indications
105 [33]. To help diversify and accelerate this process, validated open-source panels of such inhibitors,
106 such as the Public Kinase Inhibitor Set (PKIS), have been assembled for screening purposes,
107 constituting a variety of chemotypes for unbiased small molecule inhibitor discovery, which can be
108 applied to a diverse range of protein targets [34].

109 The analysis of carbohydrate sulphation currently relies heavily on genetic, biophysical (NMR) and
110 combinatorial organic chemistry and enzymatic analysis, with only a handful of low-affinity inhibitors
111 of carbohydrate sulphotransferases ever having been disclosed [13, 35]. More recently, a relatively
112 potent inhibitor of the related Type IV aryl sulphotransferase [36] and much lower affinity oestrogen
113 sulphotransferases inhibitors [37-39] were reported. Due to a lack of any selective chemical tool
114 compounds, cellular glycan sulphation remains highly understudied, relying on non-specific cellular
115 methods such as chlorate exposure [40], and the field remains ripe for technological innovation and
116 new chemical biology approaches. Early attempts to discover such molecules amongst small,
117 relatively unfocussed, kinase-based libraries led to the discovery of low-affinity purine and
118 tyrphostin-based inhibitory compounds, which are well-established chemical classes of protein kinase
119 inhibitor [35]. This raises the question as to whether PAPS-dependent sulphotransferases are general
120 inhibitory targets for new or repurposed small molecules that target nucleotide-binding sites,
121 especially broader families of compounds originally developed as protein kinase inhibitors. However,
122 the low throughput nature of radioactive (³⁵S-PAPS) TLC or HPLC-based assays typically used for
123 sulphotransferase analysis [35, 41], and the low potency of current hits, argues for new approaches to
124 assay and screen a diverse selection of chemical libraries.

125 In this paper, we describe new *in vitro* methods for assaying recombinant HS2ST, one of which

126 employs a fluorescent-based detection system with a hexasaccharide substrate. PAPS-dependent
127 sulphation of the substrate at the 2-*O* position of the IdoA residue leads to a change in substrate
128 chemical properties, which can be detected as a real-time mobility shift in a high-throughput
129 microfluidic assay format originally developed for the analysis of peptide phosphorylation [42]. We
130 exploit this assay alongside differential scanning fluorimetry (DSF) to screen a small molecule PKIS
131 library, characterising HS2ST susceptibility towards a variety of cell permeable ligands, including
132 polyanionic chemicals, the promiscuous protein kinase inhibitor rottlerin and a family of oxindole-
133 based inhibitors of the proto-oncogene RAF. We propose that appropriately validated small molecule
134 ligands might become invaluable probes for rapid cellular inhibition of HS2STs, and that further
135 iteration could lead to the synthesis (or repurposing) of small molecules, including compound classes
136 currently employed as kinase inhibitors, to probe cellular HS2ST function.

137

138

139 **EXPERIMENTAL:**

140 **MATERIALS AND METHODS:**

141 **Chemicals and Compounds**

142 Heparin or oligomeric saccharide standards, termed dp2-dp12 [43], or polymeric sulphated heparin-
143 derivatives (Table 1) were synthesised in-house as previously described [44]. *N*-sulphated,
144 fluorescein-tagged hexasaccharide glycan substrate (GlcNS-GlcA-GlcNS-IdoA-GlcNS-GlcA-
145 fluorescein, where S=sulphation) containing either L-IdoA or GlcA residues at the third residue from
146 the reducing end (to which a linker and the fluorophore were conjugated) were both purchased from
147 GLYCAN therapeutics. All standard laboratory biochemicals, were purchased from either Melford or
148 Sigma, and were of the highest analytical quality. PAPS (adenosine 3'-phosphate 5'-phosphosulphate,
149 lithium salt hydrate, APS (adenosine 5'-phosphosulphate, sodium salt), PAP (adenosine 3'-5'-
150 diphosphate, disodium salt), CoA (coenzymeA, sodium salt) dephosphoCoA (3'-dephosphoCoA,
151 sodium salt hydrate), ATP (adenosine 5'-triphosphate, disodium salt hydrate) ADP (adenosine 5'-
152 diphosphate, disodium salt), AMP (adenosine 5'-monophosphate, sodium salt), GTP (guanosine 5'-
153 triphosphate, sodium salt hydrate), GDP (guanosine 5'-diphosphate, sodium salt) or cAMP (adenosine
154 3',5'-cyclic monophosphate, sodium salt) were all purchased from Sigma and stored at -80°C to
155 minimise degradation. Rottlerin, suramin, aurintricarboxylic acid and all named kinase inhibitors were
156 purchased from Sigma, BD laboratories, Selleck or Tocris.

157 **Cloning, recombinant protein production and SDS-PAGE**

158 Chicken HS2ST (isoform 1), which exhibits ~92% identity to human HS2ST, was a kind gift from Dr
159 Lars Pedersen (NIH, USA), and was expressed in the Rosetta-gami (DE3) strain of *E. coli* from a
160 modified pMAL-c2x plasmid encoding an N-terminal Maltose Binding Protein (MBP) affinity tag.
161 Trimeric recombinant HS2ST1 enzyme was partially purified using immobilised amylose affinity
162 chromatography directly from the cleared bacterial extract, essentially as described previously [28].
163 MBP-HS2ST was eluted with maltose and further purified by SEC using a HiLoad 16/600 Superdex
164 200 column (GE Healthcare), which was equilibrated in 50 mM Tris-HCl, pH 7.4, 100 mM NaCl,
165 10% (v/v) glycerol and 1 mM DTT. Prior to analysis, purified proteins were snap frozen in liquid
166 nitrogen and stored at -80°C. This procedure generated HS2ST of >95% purity. Proteolytic removal
167 of the MBP affinity tag from HS2ST (after re-cloning with MBP and 3C protease sites into the
168 plasmid pOPINM) led to rapid HS2ST denaturation, based on rapid precipitation, so for the
169 procedures described in this paper the MBP affinity tag was left intact. For SDS-PAGE, proteins were
170 denatured in Laemmli sample buffer, heated at 95°C for 5 min and then analysed by SDS-PAGE with
171 10% (v/v) polyacrylamide gels. Gels were stained and destained using a standard Coomassie Brilliant
172 Blue protocol.

173 **DSF-based fluorescent assays**

174 Thermal shift /stability assays (TSAs) were performed using a StepOnePlus Real-Time PCR machine
175 (Life Technologies) using SYPRO-Orange dye (Emission max. 570 nm, Invitrogen), with thermal
176 ramping between 20 - 95°C in 0.3°C step intervals per data point to induce denaturation in the
177 presence or absence of test biochemicals or small molecule inhibitors, as previously described [45].
178 HS2ST was assayed at a final concentration of 5 µM in 50 mM Tris-HCl (pH 7.4) and 100 mM NaCl.
179 Final DMSO concentration in the presence or absence of the indicated concentrations of ligand was
180 no higher than 4% (v/v). Normalized data were processed using the Boltzmann equation to generate
181 sigmoidal denaturation curves, and average $T_m/\Delta T_m$ values were calculated as described using
182 GraphPad Prism software [45].

183

184 **Microfluidics-based sulphation assay**

185

186 N-sulphated, fluorescein-tagged hexasaccharide glycan substrate (GlcNS-GlcA-GlcNS-IdoA-GlcNS-
187 GlcA-fluorescein, where S=sulphation) containing either L-IdoA or D-GlcA residues at the third
188 residue from the reducing end (to which a linker and the fluorophore were conjugated) were both
189 purchased from GLYCAN therapeutics (www.glycantherapeutics.com). The fluorescein group
190 attached to the reducing end of the glycan substrate (GlcNS-GlcA-GlcNS-IdoA-GlcNS-GlcA-
191 fluorescein, where S=sulphation) possesses a maximal emission absorbance of ~525 nm, which can be
192 detected by the EZ Reader *via* LED-induced fluorescence. Heparin and heparan sulphate-derivatives
193 were generated enzymatically or through direct chemical synthesis, as described previously [4, 46].
194 Non-radioactive microfluidic mobility shift carbohydrate sulphation assays were optimised in solution
195 with a 12-sipper chip coated with SR8 reagent and a Perkin Elmer EZ Reader II system [47] using
196 EDTA-based separation buffer and real-time kinetic evaluation of substrate sulphation. Pressure and
197 voltage settings were adjusted manually to afford optimal separation of the sulphated product and
198 non-sulphated hexasaccharide substrate, with a sample (sip) volume of 20 nl, and total assay times
199 appropriate for the experiment. Individual sulphation assays were assembled in a 384 well plate in a
200 volume of 80 µl in the presence of the indicated concentration of PAPS or various test compounds, 50
201 mM HEPES, 0.015 % (v/v) Brij-35 and 5 mM MgCl₂ (unless specified otherwise). The degree of
202 oligosaccharide sulphation was directly calculated using EZ Reader software by measuring the sulpho
203 oligosaccharide:oligosaccharide ratio at each time-point. The activity of HS2ST enzymes in the
204 presence of biochemicals and small molecule inhibitors was quantified in 'kinetic mode' by
205 monitoring the amount of sulphated glycan generated over the assay time, relative to control assay
206 with no additional inhibitor molecule (DMSO control). Data was normalized with respect to these
207 control assays, with sulphate incorporation into the substrate limited to ~ 20 % to prevent depletion of
208 PAPS and to ensure assay linearity. K_m and IC_{50} values were determined by non-linear regression
209 analysis with GraphPad Prism software.

210 **NMR-based oligosaccharide sulphation analysis**

211
212 For NMR experiments, fluorescein-labelled hexasaccharide L-IdoA substrate and the HS2ST-
213 catalysed sulphation product (10 μ M) dissolved in 50 mM HEPES, pH 7.3, 5 mM MgCl₂ and 0.002%
214 (v/v) Brij-35 were lyophilised overnight and re-dissolved in an equivalent amount of D₂O. NMR
215 experiments were performed at 25°C on a Bruker Avance III 800 MHz spectrometers equipped with a
216 TCI CryoProbe. 1D and 2D proton and TOCSY spectra (mixing time 80 ms) were measured using
217 standard pulse sequences provided by the manufacturer. Spectra were processed and analysed using
218 TopSpin 3.4 software (Bruker).

219

220

221 **HPLC-based oligosaccharide sulphation analysis**

222

223 The fluorescein-labelled hexasaccharide L-IdoA substrate and the HS2ST-catalysed sulphation
224 product (10 μ M) were analyzed after anion exchange chromatography by HPLC as previously
225 described (1). Oligosaccharides were digested in the presence of a mixture of heparitinase I, II and III.
226 Samples were loaded on a Proteomix SAX-NP5 (SEPAX) column eluted with an NaCl gradient
227 Column effluent was mixed (1:1) with 2% 2-cyanoacetamide in 250mM of NaOH and subsequently
228 monitored with a fluorescence detector (JASCO; FP-1520) either at 346 nm excitation and 410 nm
229 emission (detection of mono and disaccharides linked to cyanoacetamide) or at 490 nm excitation and
230 525 nm emission for detection of trisaccharides-linked to fluorescein.

231

232 **Small molecule screening assays**

233 The PKIS chemical library (Supplementary Figure 6, designated as SB, GSK or GW compound sets)
234 comprises 367 largely ATP-competitive kinase inhibitors, covering 31 chemotypes originally
235 designed to inhibit 24 distinct protein kinase targets [48]. It was stored frozen as a 10 mM stock in
236 DMSO. The library is characterised as highly drug-like (~70% with molecular weight <500 Da and
237 clogP values <5). For initial screening, compounds dissolved in DMSO were pre-incubated with
238 HS2ST for 10 minutes and then employed for DSF or sulphotransferase-based enzyme reactions,
239 which were initiated by the addition of the universal sulphate donor PAPS. For inhibition assays,
240 competition assays, or individual IC₅₀ value determination, a compound range was prepared by serial
241 dilution in DMSO, and added directly into the assay to the appropriate final concentration. All control
242 experiments contained 4% (v/v) DMSO, which had essentially no effect on HS2ST activity.
243 Individual chemicals and glycan derivatives were prepared and evaluated using NMR, HPLC, DSF or
244 microfluidics-based assay protocols, as described above.

245

246

247 **Docking studies**

248 Docking models for rottlerin, suramin and GW407323A were built using Spartan16
249 (<https://www.wavefun.com>) and energy minimised using the Merck molecular forcefield. GOLD 5.2
250 (CCDC Software;) was used to dock molecules [49], with the binding site defined as 10 Å around the
251 5' phosphorous atom of PAP, using coordinates from chicken MBP-HS2ST PDB ID: 4NDZ [20]. A
252 generic algorithm with ChemPLP as the fitness function [50] was used to generate 10 binding-modes
253 per ligand in HS2ST. Protons were added to the protein. Default settings were retained for the “ligand
254 flexibility” and “fitness and search options”, however “GA settings” was changed to 200%.

255

256 **RESULTS:**

257 **Analysis of human HS2ST ligand binding using a thermal stability assay (TSA)**

258 To our knowledge, Differential Scanning Fluorimetry (DSF) has not previously been used to examine
259 the thermal stability and shift profiles of sulphotransferases in the presence or absence of biochemical
260 ligands, such as those related to the sulphate donor PAPS (Figure 1A). We purified recombinant
261 HS2ST catalytic domain (amino acids 69 to 356) fused to an *N*-terminal Maltose Binding Protein
262 (MBP) tag to near homogeneity (Figure 1B) and evaluated its thermal denaturation profile with the
263 MBP tag still attached in the presence of PAPS, heparin or maltose (Figure 1C). As a control, we
264 examined the profile of maltose-binding protein (MBP) incubated with the same chemicals (Figure
265 1D). Unfolding of MBP-HS2ST in buffer generated a biphasic profile, and the upper region of this
266 profile could be positively shifted (stabilised) by incubation with the HS2ST co-factor PAPS or the
267 known HS2ST-interacting oligosaccharide ligand heparin (Figure 1C). In contrast, maltose incubation
268 with MBP-HS2ST induced the same characteristic stabilisation profile observed when MBP was
269 incubated with maltose and then analysed by DSF (Figure 1D). As expected, neither PAPS nor
270 heparin induced stabilisation of MBP, confirming that effects on MBP-HS2ST were due to interaction
271 with the sulphotransferase domain, rather than the affinity tag of the recombinant protein (Figure 1D,
272 relevant ΔT_m values presented in Figure 1E). Consistently, PAPS did not stabilise the catalytic
273 domain of the ATP-dependent catalytic subunit of cAMP-dependent protein kinase (PKAc), which
274 instead binds with high affinity to the co-factor Mg-ATP [45], inducing a ΔT_m value of $>4^\circ\text{C}$ (Figure
275 1F).

276 We next analysed the sensitivity of this assay for measuring HS2ST stability shifts over a wide range
277 of PAPS concentrations, which confirmed dose-dependent stabilisation of recombinant HS2ST by
278 PAPS, with detection of binding in the low micromolar range of the co-factor, equivalent to a molar
279 ratio of $\sim 1:1$ HS2ST:PAPS (Supplementary Figure 1A). Subsequently, we explored the potential of
280 this assay to detect binding of a putative IdoA-containing oligosaccharide substrate for HS2ST,
281 confirming dose-dependent effects of this polymeric glycan over a range of concentrations, consistent
282 with binding and conformational stability. Similar to PAPS, detection of binding was observed in the
283 low micromolar range, equivalent to a molar ratio of $\sim 1:1$ HS2ST:glycan (Supplementary Figure 1B).
284 We also evaluated binding of a panel of adenine-based cofactors (PAP and ATP), which suggested
285 binding of divalent cation Mg^{2+} ions in an EDTA-sensitive manner (Supplementary Figure 1C),
286 inducing a ΔT_m of $\sim 3^\circ\text{C}$, similar to that observed with the HS2ST co-factor PAPS. In contrast,
287 removal of the sulpho moiety of PAPS, which creates the enzymatic end product PAP, was not
288 deleterious to HS2ST binding (Supplementary Figure 2A), consistent with structural analysis of the
289 enzyme [28]. Neither PAP nor PAPS binding required Mg^{2+} ions, although the effect on stabilisation
290 with Mg^{2+} ions was additive (Supplementary Figures 1C and 2A). The non-functional enzyme co-

291 factor APS, in which the 3'-phosphate group of adenine is absent, did not induce HS2ST stabilisation,
292 confirming a requirement for this charged modification (Supplementary Figure 2A). We also
293 established that CoA and acetyl CoA, which both contain a 3'-phosphoadenine moiety, clearly
294 induced thermal stabilisation of HS2ST; loss of the 3'-phosphate group in dephospho CoA abolished
295 this effect (Supplementary Figure 2A). Finally, we demonstrated that ATP, GTP and ADP, but not
296 AMP or cAMP, were all effective at protecting HS2ST from thermal denaturation, suggesting that
297 they are also HS2ST ligands (Supplementary Figure 2A).

298 **Analysis of human HS2ST glycan binding using TSA**

299 To extend our HS2ST thermal analysis to identify potential glycan substrates, we evaluated enzyme
300 stability in the presence of synthetic glycan chains of different lengths and sulphation patterns (Table
301 1). Of particular interest for further assay development, thermal shift (stabilisation) was detected in
302 this assay when hexasaccharide (dp6) or a higher degree of polymerisation oligosaccharide was
303 incubated with the enzyme (Supplementary Figure 2B), suggesting that a dp6 glycan might represent
304 the shortest potential partner suitable for HS2ST binding, a prerequisite for enzymatic modification.
305 Interestingly, highly sulphated hexameric glycans served as efficient HS2ST binding partners relative
306 to the most highly sulphated heparin control, with a fully chemically sulphated $I_{2s,3s}A^{6s}Ns$ hexamer
307 inducing the highest HS2ST stability-shift amongst the chemically-modified derivatives assessed
308 (Supplementary Figure 2C). Interestingly, a putative $I_{2OH}A^{6OH}Ns$ substrate, which contains the 2-*O*
309 moiety predicted to be the substrate for 2-*O*-sulphotransferases, also led to marked thermal
310 stabilisation of HS2ST, suggestive of productive binding to HS2ST that permit it to be sulphated in
311 the presence of PAPS (Supplementary Figure 2C).

312 **A novel microfluidic kinetic assay to directly measure oligosaccharide sulphation by HS2ST**

313 In order to quantify the effects of various ligands on HS2ST enzyme activity, we sought to develop a
314 new type of rapid non-radioactive solution assay that could discriminate the enzymatic incorporation
315 of sulphate into a synthetic oligosaccharide substrate. Current protocols are time-consuming and
316 cumbersome, requiring Mass Spectrometry, NMR or ^{35}S -based radiolabelling/HPLC separation
317 procedures. Importantly, we next tested whether a version of a $I_{2OH}A^{6OH}Ns$ hexasaccharide substrate
318 coupled to a linker and fluorescein at the reducing end, which interacts with HS2ST (Supplementary
319 Figure 2C), could also be enzymatically sulphated by HS2ST using 'gold-standard' NMR-based
320 sulphation detection [44]. The fluorescent $I_{2OH}A^{6OH}Ns$ could not be evaluated for binding to HS2ST
321 by DSF, due to interference of the fluorescent group in the unfolding assay, which measures SYPRO-
322 Orange fluorescence at a similar wavelength. Instead, to confirm sulphation of the fluorescein-
323 labelled substrate, it was pre-incubated with PAPS and HS2ST to catalyse site-specific sulphation
324 (Figure 2A). The NMR spectrum of the sulphated product compared to that of the non-modified
325 substrate provided unequivocal evidence for sulphation at the 2-*O* position of the sugar, most notably

326 due to the diagnostic shifts of anomeric H-1 and H-2 protons in the presence of the 2-*O*-sulphate
327 group linkage to the carbon atom (Figure 2B and Supplementary Figure 3). The 2-*O* sulphated IdoA
328 hexameric product was also confirmed using an established HPLC-based approach [51], which
329 demonstrated stoichiometric sulphation of an enzyme-derived substrate derivative (Supplementary
330 Figure 4).

331 Next, we evaluated the incorporation of the sulphate moiety from PAPS into a fluorescently-labelled
332 glycan substrate using a microfluidic assay that detects real-time changes in substrate covalent
333 modification (notably the introduction of a negative charge) when an electric field is applied to the
334 solution reaction. This ratiometric assay, which we and others have previously employed to detect the
335 formal double negative charge induced by real-time peptide phosphorylation [42, 52-54], was able to
336 detect real-time incorporation of sulphate into the oligosaccharide substrate, based on the different
337 retention time of the product compared to the substrate (Figure 2C). No sulphated product was
338 detected in the absence of HS2ST (Figure 2D), and prolonged incubation of substrate with HS2ST led
339 to stoichiometric conversion of the substrate into the fully sulphated product (P), which migrated very
340 differently to the substrate (S) 'marker' (Figure 2E). Analysis of product/(product + substrate) ratios
341 of the peak heights allowed us to monitor sulphation over any appropriate assay time (Figures 2F),
342 and the degree of sulphation could easily be varied as a function of PAPS concentration in the assay.
343 Furthermore, no sulphated product was detected in the presence of buffer or PAPS alone (Figure 2F),
344 allowing us to determine a K_m value of $\sim 1 \mu\text{M}$ for PAPS-mediated substrate hexasaccharide
345 sulphation (Figure 2G). We also noted that high ($>1 \text{ mM}$) concentrations of Mg^{2+} ions led to
346 concentration-dependent increases in enzyme HS2ST activity (Figure 2H), consistent with the effects
347 of Mg^{2+} ions identified in DSF assays (Supplementary Figure 2A). Finally, we confirmed that
348 sulphation was optimal when an appropriate modifiable IdoA substrate was present, with sulphation
349 reduced by $>90\%$ when a GlcA residue was incorporated into the substrate instead (compare
350 Supplementary Figures 5A and 5B).

351 **Screening for small molecule inhibitors of HS2ST using DSF and microfluidic technology**

352 The discovery of HS2ST inhibitors is hindered by a lack of a rapid and quantifiable assay for the
353 facile detection of sulphate modification using a close mimic of a physiological substrate. Our
354 discovery that a synthetic HS2ST glycan substrate could be readily sulphated and detected by
355 enzymatic assay in solution, without the need for HPLC, NMR or radioactive procedures, meant that
356 this approach might now be optimised for the discovery of small molecule HS2ST inhibitors. We first
357 evaluated the ability of an unlabelled (non-fluorescent) hexameric glycan substrate that lacked
358 sulphate at the 2-*O* position, or a non-substrate that was fully sulphated at all potential acceptor sites,
359 to act as HS2ST inhibitors in our fluorescent glycan sulphation assay. As detailed in Figure 3A, the
360 fully sulphated glycan was an extremely potent inhibitor, interfering with HS2ST-dependent

361 sulphation of the substrate with an IC_{50} value of <10 nM, consistent with tight binding to the enzyme,
362 as previously established using DSF (Supplementary Figure 2C). In contrast, a less highly sulphated
363 substrate was still able to compete with the fluorescent substrate in a dose-dependent manner (fixed at
364 $2 \mu\text{M}$ in this assay), as indicated by the IC_{50} value of <100 nM. We next compared the effects of PAP,
365 ATP, CoA and dephospho-CoA, which all exhibit thermal stabilisation of HS2ST in DSF assays
366 (Supplementary Figure 2A). Interestingly, PAP ($IC_{50} \sim 2 \mu\text{M}$), CoA ($IC_{50} = 65 \mu\text{M}$) and ATP ($IC_{50} =$
367 $466 \mu\text{M}$) were HS2ST inhibitors, whereas dephospho CoA (which lacks the 3'-phosphate moiety in
368 CoA) was not (Figure 3B). Increasing the concentration of PAPS in the assay led to a decrease in the
369 level of inhibition by both PAP and CoA (Figure 3C), suggesting a PAPS-competitive mode of
370 inhibition, as predicted from the various shared chemical features of these molecules (Figure 1A).

371 Recent studies have demonstrated that PAPS-dependent tyrosyltransferases are inhibited by several
372 non-nucleotide-based polyanionic chemicals [55]. However, to our knowledge, the inhibition of
373 carbohydrate sulphotransferases by such compounds has not been reported. Using our microfluidic
374 assay, we confirmed that the polysulphated compound suramin (an inhibitor of angiogenesis) and the
375 polyaromatic polyanion aurintricarboxylate (an inhibitor of protein:nucleic acid interactions, DNA
376 polymerase and topoisomerase II) demonstrated nanomolar inhibition of HS2ST, with IC_{50} values of
377 40 ± 1 nM and 123 ± 7 nM respectively (Figure 3D). In addition, the non-specific protein kinase
378 inhibitor rottlerin also inhibited HS2ST with an IC_{50} of $6.4 \mu\text{M}$. Increasing the concentration of PAPS
379 in the sulphation assay decreased the inhibitory effect, consistent with a competitive mode of HS2ST
380 inhibition for rottlerin (Figure 3E).

381 **Protein kinase inhibitors are a new class of potential broad-spectrum HS2ST inhibitor**

382 The finding that the non-specific kinase inhibitor rottlerin [56] was a micromolar inhibitor of HS2ST
383 was of particular interest, especially given the remarkable progress in the development of kinase
384 inhibitors as chemical probes, tool compounds and, latterly, clinically-approved drugs. Similarities
385 between ATP and PAPS (Figure 1A), and the finding that ATP can both bind to, and inhibit, HS2ST
386 activity (Supplementary Figure 2A and Figure 3B) raised the possibility that other ATP-competitive
387 protein kinase inhibitors might also interact with HS2ST. In order to exploit our screening capabilities
388 further, we established a 384-well assay to evaluate inhibition of PAPS-dependent glycan sulphation
389 by HS2ST. The Published Kinase Inhibitor Set (PKIS) is a well-annotated collection of 367 high-
390 quality ATP-competitive kinase inhibitor compounds that are ideal for compound repurposing or the
391 discovery of new chemical ligands for orphan targets. We screened PKIS using DSF and enzyme-
392 based readouts (Figures 4A and B respectively). As shown in Figure 4A, when screened at $40 \mu\text{M}$
393 compound in the presence of $5 \mu\text{M}$ HS2ST, only a small percentage of compounds induced HS2ST
394 stabilisation or destabilisation at levels similar to that seen with an ATP control. We focussed on
395 compounds inducing HS2ST ΔT_m values between $+ 0.5^\circ\text{C}$ and $- 0.5^\circ\text{C}$, and re-screened each 'hit'

396 compound using ratiometric HS2ST enzyme assays at a final compound concentration of 40 μM . We
397 reported the enzyme activity remaining compared to DMSO, with rottlerin ($\text{IC}_{50} = \sim 8 \mu\text{M}$), suramin
398 ($\text{IC}_{50} = \sim 20 \text{ nM}$) and aurintricarboxylate ($\text{IC}_{50} = \sim 90 \text{ nM}$) as positive controls (Figure 4B and
399 Supplementary Figures 6 and 7). We also included the compound GW406108X in our enzyme assay,
400 since it was structurally related to several ‘hit’ compounds from the DSF screen. As shown in Figure
401 4C, the three PKIS compounds with the highest inhibitory activity (red) exhibited IC_{50} values of
402 between 20-30 μM towards HS2ST in the presence of 1 μM PAPS, similar to inhibition by rottlerin.
403 Of particular interest, these three compounds were amongst the top ~10% of compounds in terms of
404 their ΔT_m values (red spheres, Figure 4A). Chemical deconvolution of compounds revealed that all
405 three were closely-related members of a class of oxindole-based RAF protein kinase inhibitor (Figure
406 4A). Subsequently, one other related indole RAF inhibitory compound from PKIS, GW305074, was
407 also shown to be a mid-micromolar HS2ST inhibitor, whereas the related oxindole GW405841X
408 (Supplementary Figure 7) did not inhibit HS2ST at any concentration tested. Finally, we used
409 combined DSF and enzyme assays to evaluate a broader panel of kinase inhibitors (Supplementary
410 Figure 8). However, neither the pan-kinase inhibitor staurosporine, nor several FDA-approved
411 tyrosine kinase inhibitors bound HS2ST at any concentration tested. Moreover, chemically diverse
412 RAF inhibitors, including clinical RAF compounds such as dabrafenib and vemurafenib were unable
413 to inhibit HS2ST *in vitro*, even at concentrations as high as 400 μM in our sensitive HS2ST enzyme
414 assay (Supplementary Figure 8B).

415 **Docking analysis of HS2ST ligands**

416 The X-Ray structure (PDB ID:4NDZ) of trimeric chicken MBP-HS2ST fusion protein bound to non-
417 sulphated PAP (Adenosine-3'-5'-diphosphate, a potent HS2ST inhibitor identified in this study) and
418 a polymeric oligosaccharide, have previously been reported [20, 28], and we employed a 3.45 Å
419 structural dataset to dock rottlerin, suramin and the most potent oxindole ‘hit’ (GW407323A, Figure
420 4B) from the screen, into the extended enzyme active site. As shown in Figure 5A, HS2ST possesses
421 substrate-binding features that accommodates an extended oligosaccharide that place it in close
422 proximity to the desulphated PAP end-product, which substitutes for the endogenous PAPS co-factor
423 during crystallisation. The 3'-phosphoadenine moiety of PAP also helps anchor the nucleotide in an
424 appropriate position. A molecular docking protocol for PAP in HS2ST was developed that matched
425 the crystallographic binding pose of PAP extremely well (RMSD 0.31 Å, Figure 5B). By comparing
426 a crystallised ligands (ADP) with docked rottlerin, suramin and GW407323A, we confirmed that
427 compounds could be docked into the active site of HS2ST broadly corresponding to either the PAPS-
428 binding region (rottlerin and GW407323A, Figures 5C and D) or bridging both the substrate and co-
429 factor binding sites (suramin, Figure 5E). In these binding modes, compounds make a number of
430 stabilising interactions that permit them to compete with PAPS or oligosaccharide substrate for

431 binding to HS2ST (Figure 5C). For example, rottlerin is predicted to form a hydrogen bond with the
432 amide backbone of Thr1290, GW407323A has multiple potential hydrogen bonding interactions with
433 residues including Arg1080, Asn1112 and Ser1172, whilst suramin is predicted to form hydrogen
434 bonds with residues Asn1091, Tyr1094 and Arg1288, targeting this highly elongated inhibitor to both
435 active sites.

436

437

438

439 **DISCUSSION:**

440 In this paper, we report a simple method for the detection of enzyme-catalysed glycan sulphation
441 using a model IdoA-containing hexasaccharide fused to a reducing-end fluorophore. The chemical
442 similarity between ATP, a universal phosphate donor, and PAPS, a universal sulphate donor, led us to
443 investigate whether enzymatic glycan sulphation could be detected using a high-throughput kinetic
444 procedure previously validated for peptide phosphorylation by ATP-dependent protein kinases. We
445 focussed our attention on HS2ST, which transfers sulphate from PAPS to the 2-*O* position of IdoA
446 during heparan sulphate biogenesis in the secretory pathway.

447 To facilitate rapid purification of recombinant HS2ST, the enzyme was expressed as an N-terminal
448 MBP fusion protein, and we confirmed that it was folded, and could bind to a variety of exogenous
449 ligands including PAPS and PAP, the end product of the sulphotransferase reaction. Protein kinases
450 are also known to bind to their end product (ADP), and kinase structural analysis has long taken
451 advantage of the stability of kinase and ADP complexes for protein co-crystallisation. Similar co-
452 crystallisation approaches revealed the structure of HS2ST, and related sulphotransferases, in complex
453 with PAP and model saccharide substrates [20, 21], and our study extends these approaches, by
454 revealing a competitive mode of HS2ST interaction with a variety of 3'-phosphoadenosine-containing
455 nucleotides, including Coenzyme A (CoA). They also suggest that generalised docking of a
456 3'-phosphoadenosine moiety is a feature of HS2ST that could be mimicked using other small molecule
457 inhibitors. DSF-based thermal shift assays are ideal for the analysis of a variety of proteins and
458 ligands, including growth factors [4, 57], protein kinase domains [45, 54, 58], pseudokinase domains
459 [59], BH3 [60] and bromodomain-containing proteins [61]. However, to our knowledge, this is the
460 first report to demonstrate the utility of a DSF-based strategy for the analysis of a sulphotransferase.

461 **Competitive HS2ST inhibition by biochemical ligands**

462 By developing a new type of rapid, kinetic glycan sulphation assay, we confirmed that many HS2ST
463 ligands also act as competitive inhibitors of PAPS-dependent oligosaccharide sulphation, setting the
464 stage for a broader screening approach for the discovery of HS2ST inhibitors. Standard assays for
465 carbohydrate sulphation utilise HPLC-based detection of ³⁵S-based substrate sulphation derived from
466 ³⁵S-labelled PAPS, requiring enzymatic co-factor synthesis and time-consuming radioactive solid-
467 phase chromatography procedures [20, 35, 41]. Whilst enzymatic deconvolution, MS and NMR-based
468 procedures remain useful for mapping sulphation patterns in complex (sometimes unknown) glycan
469 polymers, these procedures are very time-consuming and relatively expensive. In contrast, our finding
470 that sulphation can be detected using a simple glycan mobility shift assay, and then quantified in real
471 time by comparing the ratio of a sulphated and non-sulphated substrate, is rapid, reproducible and
472 highly cost effective. Our kinetic assay makes use of a commercial platform originally developed for
473 the analysis of peptide phosphorylation or peptide proteolysis, which allows for the inclusion of high

474 concentrations of non-radioactive co-factors, substrates and ligands in assays [58]. Consequently, we
475 were able to use this technology to derive a K_m value for PAPS in our standard HS2ST assay of 1.0
476 μM (Figure 2G), slightly lower than the reported literature value of 18.5 μM for HS2ST using
477 desulphated heparin as substrate [20], but similar to the reported literature value of ~ 4.3 μM for the
478 PAPS-dependent GlcNAc-6-sulphotransferase NodH from *Rhizobium melitoli* [35] and 1.5 and 10
479 μM for human hormone iodothyrosine sulphotransferases and tissue-purified tyrosyl
480 sulphotransferase [62, 63]. In the course of our studies, we developed several new reagents, including
481 a hexameric fluorescent substrate in which the IdoA residue was replaced by a GlcA residue
482 (Supplementary Figure 4). Interestingly, a decreased rate of substrate modification was observed
483 using this oligosaccharide substrate, consistent with the ability of HS2ST to sulphate either IdoA or
484 GlcA [19], but with a preference for the former. Previous HPLC-based studies identified an N-sulpho
485 group in the oligosaccharide substrate as a pre-requisite for catalysis, with subsequent preferential
486 transfer of sulphate to the 2-*O* position of IdoA [20, 22, 28, 64]; these published observations are
487 entirely consistent with our findings using a hexameric fluorescent substrate.

488 In the future, it might be possible to quantify other site-specific covalent modifications in complex
489 glycans using fluorescent oligosaccharides that contain distinct sugar residues, and by employing
490 mobility-dependent detection in the presence of a variety of enzymes. These could include 3-*O* and 6-*O*
491 sulphotransferases [21] or structurally distinct glycan phosphotransferases, such as the protein-*O*-
492 mannose kinase POMK/Sgk196 [65], which catalyses an essential phosphorylation step during
493 biosynthesis of an α -dystroglycan substrate [66]. Using this general approach, the screening and
494 comparative analysis of small molecule inhibitors of these distinct enzyme classes would be
495 simplified considerably relative to current procedures.

496 **HS2ST inhibition by previously known kinase inhibitors, including a family of RAF inhibitor**

497 Our finding that HS2ST was inhibited at sub-micromolar concentrations by the compounds suramin
498 [67] and the DNA polymerase inhibitor aurintricarboxylic acid [68] was intriguing, and consistent
499 with recent reports demonstrating inhibitory activity of these compounds towards tyrosyl protein
500 sulphotransferases, which employ PAPS as a co-factor, but instead sulphate tyrosine residues in
501 proteins [55]. During the course of our studies screening a panel of kinase inhibitors, we found that
502 the non-specific kinase compound rottlerin is a low micromolar inhibitor of HS2ST *in vitro*, with
503 inhibition dependent upon the concentration of PAPS in the assay, suggesting a competitive mode of
504 interaction. Rottlerin (also known as mallotoxin) is a polyphenolic compound from *Mallotus*
505 *philippensis*, and although originally identified as an inhibitor of PKC isozymes [69], possesses a
506 wide variety of biological effects likely due to its non-specific inhibition of multiple protein kinases
507 [56]. This lack of specificity prevents exploitation of rottlerin in cells as a specific probe, although our
508 finding that HS2ST is a target of this compound opens up the possibility that this, or other, protein

509 kinase inhibitors might also possess inhibitory activity towards HS2ST, either due to an ability to
510 target the PAPS or oligosaccharide-binding sites in the enzyme. To evaluate these possibilities further,
511 we screened PKIS, a collection of drug-like molecules with broad inhibitory activity towards multiple
512 protein kinases. Interestingly, only 3 compounds (<1% of the library) consistently showed marked
513 inhibitory activity at 40 μ M in our HS2ST enzyme assay (Figure 4A, B and C, red). Remarkably, all
514 three compounds belonged to the same benzylidene-1H-inol-2-one (oxindole) chemical class, which
515 were originally reported as potent ATP-dependent RAF kinase inhibitors that block the MAPK
516 signalling pathway in cultured cells [70]. Retrospectively, of all the related chemotypes present in the
517 PKIS library, we confirmed that GW305074X (but not GW405841X) was also a low micromolar
518 HS2ST inhibitor, consistent with the broad sensitivity of HS2ST to this optimised class of RAF
519 inhibitor.

520 Although limited Structure Activity Relationships can be derived from our initial studies, these
521 findings demonstrate that HS2ST inhibitors can be discovered, and that several of these inhibitors
522 could be of broad interest to the sulphotransferase (and protein kinase) fields. Our study also validates
523 previous observations from the turn of the century, in which carbohydrate inhibitors of NoDH
524 sulphotransferase were reported from a low diversity kinase-directed library [35]. Surprisingly, this
525 early breakthrough did not lead to the development of any glycan sulphotransferase tool compounds
526 for cell-based analysis. However, our discovery that oxindole-based RAF inhibitors are also HS2ST
527 inhibitors could provide new impetus for the design and synthesis of much more specific and potent
528 HS2ST inhibitors from this class of RAF kinase inhibitor. A requirement for rapid progress during
529 this process will be structure-based analysis of HS2ST in the presence of compounds, in order to
530 determine mechanism and mode(s) of interaction. Our initial docking studies suggest similar binding
531 modes for both rottlerin and the oxindole-based ligand GW407323A (Figure 5), with the potential for
532 cross-over between PAPS and substrate-binding sites present on the surface of HS2ST. It will be
533 intriguing to explore these binding modes by structural analysis and guided mutational approaches
534 [71], to evaluate potential drug-binding site residues in HS2ST and tease-apart requirements for
535 enzyme inhibition. It will also be important to evaluate whether compounds identified as *in vitro*
536 HS2ST inhibitors, including RAF inhibitors, can also interfere with HS sulphation and downstream
537 signalling in cells. Interestingly, suramin is a potent anti-angiogenic compound, and is reported to
538 have cellular effects on FGF signalling [72], whereas aurintricarboxylate has multiple cellular effects
539 currently attributed to nucleotide-dependent processes; attempting to link some of these cellular
540 phenotypes to the inhibition of glycan sulphation is also a worthy experimental strategy.

541

542 **CONCLUSION:**

543 Our work raises the possibility that HS2ST inhibitors could be strategically developed following the
544 successful blueprint laid down for protein kinase inhibitors in the previous decades. Dozens of
545 sulphotransferases are found in vertebrate genomes, and the development of chemical biology
546 approaches to rapidly inactivate Golgi membrane-bound sulphotransferases and induce targeted
547 inhibition of sulphation has been stymied by a lack of tool compounds, which have the opportunity to
548 revolutionise cell biology when properly validated [73, 74]. We propose that if such compounds can
549 be developed, perhaps by the discovery of new inhibitors, or through chemical manipulation of the
550 leads reported in this study, then a new era in sulphation-based cell biology might be on the horizon.
551 By generating tools to chemically control glycan sulphation modulated by HS2ST directly, inhibitor-
552 based interrogation of sulphation-dependent enzymes could also have significant impact in many
553 active areas of translational research.

554 **ACKNOWLEDGEMENTS:**

555 This work was funded by a BBSRC Tools and Resources Development Grant (BB/N021703/1) and a
556 Royal Society Research Grant (to PAE), a European Commission FET-OPEN grant (ArrestAD
557 no.737390) to DPG, SC, DGF and PAE, North West Cancer Research (NWCR) grants CR1088 and
558 CR1097 and a NWCR endowment (to DGF). VP is supported by NIH Small Business Innovation
559 Research Contract HHSN261201500019C. The SGC is a registered charity (number 1097737) that
560 receives funds from AbbVie, Bayer Pharma AG, Boehringer Ingelheim, Canada Foundation for
561 Innovation, Eshelman Institute for Innovation, Genome Canada, Innovative Medicines Initiative
562 (EU/EFPIA) [ULTRA-DD grant no. 115766], Janssen, Merck KGaA Darmstadt Germany, MSD,
563 Novartis Pharma AG, Ontario Ministry of Economic Development and Innovation, Pfizer, São Paulo
564 Research Foundation-FAPESP, Takeda, and The Wellcome Trust [106169/ZZ14/Z].

565 **AUTHOR CONTRIBUTIONS**

566 PAE obtained BBSRC grant funding with DGF and EAY. PAE, DPB, EAY, ILB, CEE, DPG, SC and
567 NGB designed and executed the experiments. VP, JL, CW, DHD and WJZ provided critical reagents,
568 compound libraries, protocols and critical advice. PAE wrote the paper with contributions and final
569 approval from all of the co-authors.

570

571 **FIGURE LEGENDS:**

572 **Figure 1. Analysis of purified recombinant MBP-HS2ST protein.**

573 (A) Structures of PAPS and PAPS-related biochemicals. (B) Coomassie blue staining of recombinant
574 MBP-HS2ST1 protein. ~2 µg of purified enzyme was analysed after SDS-PAGE. (C) Thermal
575 denaturation profiles of MBP-HS2ST (5 µM) and thermal shift in the presence of 0.5 mM PAPS (red),
576 10 µM heparin (blue) or 5 mM maltose (green). Buffer control is shown in black dashed lines. (D)
577 Thermal denaturation profile of purified recombinant maltose binding protein (MBP). Experimental
578 conditions as for (C). (E) T_m values measured for 5 µM MBP (squares) or MBP-HS2ST fusion protein
579 (triangles) in the presence of 0.5 mM PAPS, 10 µM heparin or 5 mM maltose. ΔT_m values were
580 obtained by DSF and calculated by subtracting control T_m values (buffer, no ligand) from the
581 measured T_m . (F) ΔT_m values relative to buffer addition for recombinant PKAc (5 µM) measured in
582 the presence of 0.5 mM PAPS, 0.5 mM ATP or 0.5 mM ATP and 10 mM $MgCl_2$. Similar results were
583 seen in three independent experiments.

584

585 **Figure 2. Development of a novel microfluidic mobility shift assay to quantify HS2ST enzymatic**
586 **activity.**

587 (A) Schematic showing PAPS-dependent sulphate incorporation into the fluorescein-labelled
588 hexasaccharide IdoA substrate by HS2ST, with the concomitant generation of PAP. R=fluorescein.
589 (B) NMR analysis of the non-sulphated and sulphated hexasaccharides. The addition of a 2-O-
590 sulphate group to the iduronate (L-IdoA) residue of the fluorescent hexasaccharide results in a
591 significant chemical shift change, most notably to the anomeric proton (H-1) and that of H-2 attached
592 to the sulphated carbon atom of L-IdoA, in agreement with expected values from the literature [44]. 1H
593 NMR spectrum of non-sulphated substrate (bottom spectrum, black) and sulphated product (upper
594 spectrum, red). Distinct L-IdoA protons (H-3 and H-4 of the spin system) were identified by TOCSY
595 and are shown vertically above their respective H-1 signals (for the non-sulphated substrate, right blue
596 boxed, and for the sulphated product, left blue boxed). The full carbohydrate proton spectra are shown
597 in Supplementary Figure 3. (C, D) Screen shots of EZ reader II raw data files, demonstrating that
598 HS2ST induces a rapid mobility change in the IdoA-containing fluorescent hexasaccharide.
599 Separation of the higher mobility, sulphated (product, P) from the lower mobility (substrate, S)
600 hexasaccharide occurs as a result of enzymatic substrate sulphation (left panels 180 s assay time, right
601 panels 240 s assay time), as demonstrated by omission of HS2ST from the assay (-HS2ST). Assays
602 were initially performed at 20°C using 90 nM of purified HS2ST, 2 µM fluorescein-labelled
603 hexasaccharide substrate and 500 µM PAPS. (E) Stoichiometric sulphate-labelling of IdoA-containing
604 fluorescein-labelled hexasaccharide. Reactions was performed with 0.6 µM HS2ST, 375 µM IdoA-
605 hexasaccharide substrate and 1 mM PAPS and incubated at room temperature for 48 h. The reaction
606 was spiked with an additional 0.5 mM (final concentration) of PAPS after 24 h of incubation. M =

607 non-sulphated marker substrate. A final hexasaccharide concentration of 2 μM was analysed by
608 fluorescent sulphation mobility assay. **(F)** Analysis of time-dependent sulphate incorporation into 2
609 μM IdoA-containing fluorescein-conjugated hexasaccharide. Percentage sulphation was calculated
610 from the ratio of substrate hexasaccharide to product (2-*O*-sulpho)-hexasaccharide at the indicated
611 time points in the presence or absence of 20 nM HS2ST and 10 μM PAPS. **(G)** Calculation of K_m
612 [PAPS] value for HS2ST. PAPS concentration was varied in the presence of a fixed concentration of
613 HS2ST (20 nM), and the degree of substrate sulphation calculated from a differential kinetic analysis,
614 $n=2$ assayed in duplicate. **(H)** Duplicate HS2ST assays conducted in the presence of increasing
615 concentrations of activating Mg^{2+} ions. Activity is presented in duplicate relative to buffer controls.
616 Similar results were seen in several independent experiments.

617

618 **Figure 3. Microfluidic sulphotransferase assay to measure inhibition of HS2ST activity *in vitro*.**

619 Assays were performed using 20 nM HS2ST and the extent of substrate sulphation was determined
620 after 15 mins incubation at room temperature as described in the legend to Figure 2. Dose-response
621 curves for inhibition of HS2ST activity by **(A)** modified heparin derivatives containing different
622 sulphation patterns (assayed in the presence of 0.5 mM MgCl_2) or **(B)** nucleotides (assayed in the
623 absence of MgCl_2). Assays contained HS2ST and 10 μM PAPS and the indicated concentration of
624 inhibitory ligand or buffer. **(C)** Inhibition of HS2ST activity by fixed 10 μM PAP, 0.5 mM CoA or
625 0.5 mM dephospho-CoA in the presence of increasing concentration of PAPS. Inhibition is calculated
626 as a function of no inhibitor for each concentration of PAPS in the absence of MgCl_2 . **(D)** Evaluation
627 of small molecule HS2ST inhibitory profiles in the presence of 10 μM PAPS. **(E)** Inhibition HS2ST
628 activity by 20 μM rottlerin in the presence of varied concentrations of PAPS, suggesting a competitive
629 mode of inhibition. Similar results were seen in multiple experiments.

630

631 **Figure 4. Mining the PKIS inhibitor library for HS2ST inhibitor compounds.**

632 **(A)** Evaluation of small molecule ligands in a high-throughput HS2ST DSF assay. 5 μM HS2ST was
633 screened in the presence or absence of 20 μM compound. The final concentration of DMSO in the
634 assay was 4 % (v/v). ΔT_m values (positive and negative) were calculated by subtracting the control T_m
635 value (DMSO alone) from the measured T_m value. Data shown on a scatter plot of the mean ΔT_m
636 values from two independent DSF assays. **(B)** Enzymatic analysis of HS2ST inhibition by selected
637 PKIS compounds. HS2ST (20 nM) was incubated with the indicated PKIS compound (40 μM) in the
638 presence of 10 μM PAPS for 15 mins at room temperature. HS2ST sulphotransferase activity was
639 assayed using the fluorescent hexasaccharide substrate and normalised to DMSO control (4 % v/v).
640 **(C)** Full dose-response curves for selected compounds. HS2ST (20 nM) was incubated with
641 increasing concentration of inhibitor in the presence of 1 μM PAPS for 15 mins at 20°C. HS2ST
642 activity calculated as above. Data from two independent experiments are combined. Similar results
643 were seen in two independent experiments.

644 **Figure 5. Molecular docking analysis of HS2ST with small molecule inhibitor compounds.**

645 (A) Structural representation of the catalytic domain of chicken MBP-HS2ST crystallised with bound
646 heptasaccharide and non-sulphated PAP co-factor (Protein rendered as a cartoon. Red – α helix,
647 yellow – β sheet, green – loop. PAP (Adenosine-3'-5'-diphosphate) and heptasaccharide are rendered
648 as coloured sticks. Grey – carbon, red, oxygen, blue – nitrogen, yellow – sulphur. Black dotted line
649 indicates close proximity of glycan 2-OH group and PAP. (B) Structure of HS2ST with near identical
650 crystallographic (carbons in cyan) and docking (carbons in purple) poses of PAP (Protein rendered as
651 a cartoon. Red – α helix, yellow – β sheet, green – loop. PAP rendered as coloured sticks.
652 Cyan/Grey/Purple – carbon, red, oxygen, blue – nitrogen, dark yellow – sulphur). Black dotted lines
653 indicate hydrogen bonds. Molecular Docking of (C) rottlerin, (D) the indole RAF inhibitor
654 GW407323A or (E) suramin into the HS2ST catalytic domain (Protein depicted as a cartoon. Red – α
655 helix, yellow – β sheet, green – loop. Docked molecules coloured as sticks. Pink/Yellow/Salmon/Grey
656 – carbon, red, oxygen, blue – nitrogen, dark yellow – sulphur, white – hydrogen). Black dotted lines
657 indicate hydrogen bonds).

658 **Supplementary Figure 1. Thermal stability analysis of MBP-HS2ST.**

659 Concentration-dependent thermal profiling of MBP-HS2ST in the presence of (A) PAPS and the
660 chemically-modified heparin derivative $I_{2OH}A^{60H}N_S$ (compound 7, see Table 1). (B) TSA of 5 μ M
661 MBP-HS2ST measured in the presence of the indicated concentration of PAPS or $I_{2OH}A^{60H}N_S$. ΔT_m
662 values were calculated by DSF as previously described. (C) TSA assay showing changes in MBP-
663 HS2ST thermostability induced by PAP and ATP, and the effects of EDTA and Mg^{2+} . Thermal
664 stability of HS2ST was measured as a function of compound binding by DSF. ΔT_m values of HS2ST
665 protein (5 μ M) incubated with 0.5 mM of the indicated nucleotide \pm 10 mM $MgCl_2 \pm$ 10 mM EDTA
666 are shown. (Describe Colours)

667

668 **Supplementary Figure 2. MBP-HS2ST Nucleotide and polysaccharide analysis.**

669 (A) TSA showing MBP-HS2ST binding of nucleotides by DSF. Thermal stability was measured as a
670 function of nucleotide binding by DSF. ΔT_m values of HS2ST protein (5 μ M) incubated with 0.5 mM
671 of the indicated nucleotide \pm 10 mM $MgCl_2$ are shown. DSF analysis showing thermal shift
672 (stabilization) of 5 μ M HS2ST in the presence of 10 μ M size separated oligosaccharide fragments, dp
673 (degree of polymerisation) equivalent to disaccharide (dp2), tetrasaccharide (dp4), hexasaccharide
674 (dp6), octasaccharide (dp8), decaasaccharide (dp10) or dodecasaccharide (dp12) (B) or chemically-
675 modified heparin derivatives (C). The minimal hexasaccharide binding substrate in (B) and the
676 putative HS2ST substrate $I_{2OH}A^{60H}N_S$ in (C) are both shown in red. ΔT_m values (calculated as
677 previously described) are normalized relative to heparin. dp=degree of polymerisation.

678

679 **Supplementary Figure 3. NMR spectra of sulphated and non-sulphated fluorescent**
680 **polysaccharide substrate.**

681 TOCSY spectra of the L-IdoA-containing hexameric fluorescein-labelled HS2ST substrate (top) and
682 the 2-O-sulphated product (bottom) generated by incubation with HS2ST, including the full spectrum
683 of all carbohydrate hydrogens detected. Selected spectral regions, including the diagnostic shift
684 caused by 2-O-sulphation, are expanded in Figure 2B in the main text, and are highlighted here by
685 black and red boxes respectively.

686

687 **Supplementary Figure 4. HPLC analysis of sulphated and non-sulphated fluorescent**
688 **polysaccharide substrate.**

689 HPLC separation of cyanoacetamide or fluorescein-labelled saccharides obtained from heparitinase
690 digestion of GlcNS-GlcA-GlcNS-IdoA-GlcNS-GlcA-Fluorescein HS2ST substrate. Elution profiles
691 of digested polysaccharide after anion exchange chromatography are shown. The non-sulphated IdoA-
692 containing hexameric substrate (eluting at ~34 min, top) and the 2-O-sulphated product (eluting at
693 ~37 min, bottom) were confirmed by comparison of the different peaks in the fluorescence spectra
694 (dashed lines), with the later eluting sulphated product highlighted in red. dIdoA refers to the double
695 bond formed by β -elimination between C4 and C5 in the IdoA and 2-O-IdoA oligosaccharides.

696

697 **Supplementary Figure 5. HS2ST glycan residue substrate-specificity analysis.**

698 Efficient sulphation of a hexasaccharide substrate by HS2ST requires an L-IdoA residue at the
699 appropriate position in the oligosaccharide. Direct microfluidic sulphotransferase assays
700 demonstrating time-dependent sulphation of the fluorescein-tagged hexasaccharide substrate
701 containing either (A) L-IdoA or (B) D-GlcA residue at the third residue from the fluorescein-
702 conjugated (reducing) end. R=fluorescein. The IdoA or GlcA residues are indicated in red.

703

704 **Supplementary Figure 6. HS2ST enzymatic PKIS compound screen.**

705 Inhibition of HS2ST catalytic activity by selected PKIS members. Data are presented as HS2ST
706 activity relative to DMSO control, assayed in duplicate. The most notable 'hit' inhibitors from the
707 oxindole chemical class are shaded in red.

708

709 **Supplementary Figure 7. Chemical structures of HS2ST inhibitory ligands.**

710 Chemical structures of surmain, rottlerin, aurintricarboxylic acid and selected PKIS compounds.

711

712 **Supplementary Figure 8. Lack of HS2ST inhibition by various kinase inhibitors.**

713 DSF screening (left panel) or enzyme-based inhibitor assay (right panel) evaluating staurosporine,
714 FDA-approved kinase inhibitors and several chemically-distinct RAF kinase inhibitors.

715

716 **Table 1.**
 717 **Predominant substitution patterns of differentially-sulphated heparin derivatives described in**
 718 **this study.**

Analogue	Predominant repeat	IdoUA-2	GlcN-6	GlcN-2	IdoUA-3	GlcN-3a
1 (Heparin)	I ₂ S A ^{6S} Ns	SO ₃ ⁻	SO ₃ ⁻	SO ₃ ⁻	OH	OH
2	I ₂ S A ^{6S} NAc	SO ₃ ⁻	SO ₃ ⁻	COCH ₃	OH	OH
3	I ₂ OH A ^{6S} Ns	OH	SO ₃ ⁻	SO ₃ ⁻	OH	OH
4	I ₂ S A ^{6OH} Ns	SO ₃ ⁻	OH	SO ₃ ⁻	OH	OH
5	I ₂ OH A ^{6S} NAc	OH	SO ₃ ⁻	COCH ₃	OH	OH
6	I ₂ S A ^{6OH} NAc	SO ₃ ⁻	OH	COCH ₃	OH	OH
7	I ₂ OH A ^{6OH} Ns	OH	OH	SO ₃ ⁻	OH	OH
8	I ₂ OH A ^{6OH} NAc	OH	OH	COCH ₃	OH	OH
9	I ₂ S ₃ S A ^{6S} ₃ S Ns	SO ₃ ⁻	SO ₃ ⁻	SO ₃ ⁻	SO ₃ ⁻	SO ₃ ⁻

719

720

721

722

723

724

725

726

727

728

729

730

731 **REFERENCES:**

732

- 733 1. Leung, A.W., I. Backstrom, and M.B. Bally, *Sulfonation, an underexploited area: from*
734 *skeletal development to infectious diseases and cancer*. *Oncotarget*, 2016. **7**(34): p. 55811-
735 55827.
- 736 2. Bowman, K.G. and C.R. Bertozzi, *Carbohydrate sulfotransferases: mediators of extracellular*
737 *communication*. *Chemistry & biology*, 1999. **6**(1): p. R9-R22.
- 738 3. Kreuger, J., et al., *Interactions between heparan sulfate and proteins: the concept of*
739 *specificity*. *The Journal of cell biology*, 2006. **174**(3): p. 323-7.
- 740 4. Li, Y., et al., *Heparin binding preference and structures in the fibroblast growth factor family*
741 *parallel their evolutionary diversification*. *Open biology*, 2016. **6**(3).
- 742 5. Tillo, M., et al., *2- and 6-O-sulfated proteoglycans have distinct and complementary roles in*
743 *cranial axon guidance and motor neuron migration*. *Development*, 2016. **143**(11): p. 1907-
744 13.
- 745 6. Chan, W.K., D.J. Price, and T. Pratt, *FGF8 morphogen gradients are differentially regulated*
746 *by heparan sulphotransferases Hs2st and Hs6st1 in the developing brain*. *Biology open*,
747 2017. **6**(12): p. 1933-1942.
- 748 7. Clegg, J.M., et al., *Heparan sulfotransferases Hs6st1 and Hs2st keep Erk in check for mouse*
749 *corpus callosum development*. *The Journal of neuroscience : the official journal of the Society*
750 *for Neuroscience*, 2014. **34**(6): p. 2389-401.
- 751 8. Chan, W.K., et al., *2-O Heparan Sulfate Sulfation by Hs2st Is Required for Erk/Mapk*
752 *Signalling Activation at the Mid-Gestational Mouse Telencephalic Midline*. *PLoS one*, 2015.
753 **10**(6): p. e0130147.
- 754 9. Kreuger, J., et al., *Sequence analysis of heparan sulfate epitopes with graded affinities for*
755 *fibroblast growth factors 1 and 2*. *The Journal of biological chemistry*, 2001. **276**(33): p.
756 30744-52.
- 757 10. Rosen, S.D. and C.R. Bertozzi, *Two selectins converge on sulphate*. *Leukocyte adhesion*.
758 *Current biology : CB*, 1996. **6**(3): p. 261-4.
- 759 11. Sanders, W.J., et al., *L-selectin-carbohydrate interactions: relevant modifications of the*
760 *Lewis x trisaccharide*. *Biochemistry*, 1996. **35**(47): p. 14862-7.
- 761 12. Sepulveda-Diaz, J.E., et al., *HS3ST2 expression is critical for the abnormal phosphorylation*
762 *of tau in Alzheimer's disease-related tau pathology*. *Brain : a journal of neurology*, 2015.
763 **138**(Pt 5): p. 1339-54.
- 764 13. Armstrong, J.I. and C.R. Bertozzi, *Sulfotransferases as targets for therapeutic intervention*.
765 *Current opinion in drug discovery & development*, 2000. **3**(5): p. 502-15.
- 766 14. Williams, S.J., *Sulfatase inhibitors: a patent review*. *Expert opinion on therapeutic patents*,
767 2013. **23**(1): p. 79-98.
- 768 15. Lanzi, C., N. Zaffaroni, and G. Cassinelli, *Targeting Heparan Sulfate Proteoglycans and their*
769 *Modifying Enzymes to Enhance Anticancer Chemotherapy Efficacy and Overcome Drug*
770 *Resistance*. *Current medicinal chemistry*, 2017. **24**(26): p. 2860-2886.
- 771 16. Chapman, E., et al., *Sulfotransferases: structure, mechanism, biological activity, inhibition,*
772 *and synthetic utility*. *Angewandte Chemie*, 2004. **43**(27): p. 3526-48.
- 773 17. Kakuta, Y., et al., *Conserved structural motifs in the sulfotransferase family*. *Trends in*
774 *biochemical sciences*, 1998. **23**(4): p. 129-30.
- 775 18. Kinnunen, T., et al., *Heparan 2-O-sulfotransferase, hst-2, is essential for normal cell*
776 *migration in Caenorhabditis elegans*. *Proceedings of the National Academy of Sciences of*
777 *the United States of America*, 2005. **102**(5): p. 1507-12.
- 778 19. Rong, J., et al., *Substrate specificity of the heparan sulfate hexuronic acid 2-O-*
779 *sulfotransferase*. *Biochemistry*, 2001. **40**(18): p. 5548-55.
- 780 20. Liu, C., et al., *Molecular mechanism of substrate specificity for heparan sulfate 2-O-*
781 *sulfotransferase*. *The Journal of biological chemistry*, 2014. **289**(19): p. 13407-18.
- 782 21. Liu, J., et al., *Understanding the substrate specificity of the heparan sulfate sulfotransferases*
783 *by an integrated biosynthetic and crystallographic approach*. *Current opinion in structural*
784 *biology*, 2012. **22**(5): p. 550-7.

- 785 22. Xu, D., et al., *Mutational study of heparan sulfate 2-O-sulfotransferase and chondroitin*
786 *sulfate 2-O-sulfotransferase*. The Journal of biological chemistry, 2007. **282**(11): p. 8356-67.
- 787 23. Lamanna, W.C., et al., *Sulf loss influences N-, 2-O-, and 6-O-sulfation of multiple heparan*
788 *sulfate proteoglycans and modulates fibroblast growth factor signaling*. The Journal of
789 biological chemistry, 2008. **283**(41): p. 27724-35.
- 790 24. Merry, C.L., et al., *The molecular phenotype of heparan sulfate in the Hs2st^{-/-} mutant mouse*.
791 The Journal of biological chemistry, 2001. **276**(38): p. 35429-34.
- 792 25. Wilson, V.A., J.T. Gallagher, and C.L. Merry, *Heparan sulfate 2-O-sulfotransferase (Hs2st)*
793 *and mouse development*. Glycoconjugate journal, 2002. **19**(4-5): p. 347-54.
- 794 26. Merry, C.L. and V.A. Wilson, *Role of heparan sulfate-2-O-sulfotransferase in the mouse*.
795 Biochimica et biophysica acta, 2002. **1573**(3): p. 319-27.
- 796 27. Esko, J.D., C. Bertozzi, and R.L. Schnaar, *Chemical Tools for Inhibiting Glycosylation*, in
797 *Essentials of Glycobiology*, rd, et al., Editors. 2015: Cold Spring Harbor (NY). p. 701-712.
- 798 28. Bethea, H.N., et al., *Redirecting the substrate specificity of heparan sulfate 2-O-*
799 *sulfotransferase by structurally guided mutagenesis*. Proceedings of the National Academy of
800 Sciences of the United States of America, 2008. **105**(48): p. 18724-9.
- 801 29. Madhusudan, et al., *cAMP-dependent protein kinase: crystallographic insights into substrate*
802 *recognition and phosphotransfer*. Protein science : a publication of the Protein Society, 1994.
803 **3**(2): p. 176-87.
- 804 30. Teramoto, T., et al., *Crystal structure of human tyrosylprotein sulfotransferase-2 reveals the*
805 *mechanism of protein tyrosine sulfation reaction*. Nature communications, 2013. **4**: p. 1572.
- 806 31. Cohen, P., *Protein kinases--the major drug targets of the twenty-first century?* Nature
807 reviews. Drug discovery, 2002. **1**(4): p. 309-15.
- 808 32. Zhang, J., P.L. Yang, and N.S. Gray, *Targeting cancer with small molecule kinase inhibitors*.
809 Nature reviews. Cancer, 2009. **9**(1): p. 28-39.
- 810 33. Ferguson, F.M. and N.S. Gray, *Kinase inhibitors: the road ahead*. Nature reviews. Drug
811 discovery, 2018.
- 812 34. Drewry, D.H., et al., *Progress towards a public chemogenomic set for protein kinases and a*
813 *call for contributions*. PloS one, 2017. **12**(8): p. e0181585.
- 814 35. Armstrong, J.I., et al., *Discovery of Carbohydrate Sulfotransferase Inhibitors from a Kinase-*
815 *Directed Library*. Angewandte Chemie, 2000. **39**(7): p. 1303-1306.
- 816 36. Chapman, E., et al., *A potent and highly selective sulfotransferase inhibitor*. Journal of the
817 American Chemical Society, 2002. **124**(49): p. 14524-5.
- 818 37. Armstrong, J.I., D.E. Verdugo, and C.R. Bertozzi, *Synthesis of a bisubstrate analogue*
819 *targeting estrogen sulfotransferase*. The Journal of organic chemistry, 2003. **68**(1): p. 170-3.
- 820 38. Verdugo, D.E., et al., *Discovery of estrogen sulfotransferase inhibitors from a purine library*
821 *screen*. Journal of medicinal chemistry, 2001. **44**(17): p. 2683-6.
- 822 39. Armstrong, J.I., et al., *A library approach to the generation of bisubstrate analogue*
823 *sulfotransferase inhibitors*. Organic letters, 2001. **3**(17): p. 2657-60.
- 824 40. Baeuerle, P.A. and W.B. Huttner, *Chlorate--a potent inhibitor of protein sulfation in intact*
825 *cells*. Biochemical and biophysical research communications, 1986. **141**(2): p. 870-7.
- 826 41. Bourdineaud, J.P., et al., *Enzymatic radiolabelling to a high specific activity of legume lipo-*
827 *oligosaccharidic nodulation factors from Rhizobium meliloti*. The Biochemical journal, 1995.
828 **306** (Pt 1): p. 259-64.
- 829 42. Mohanty, S., et al., *Hydrophobic Core Variations Provide a Structural Framework for*
830 *Tyrosine Kinase Evolution and Functional Specialization*. PLoS genetics, 2016. **12**(2): p.
831 e1005885.
- 832 43. Linhardt, R.J., et al., *Structure and activity of a unique heparin-derived hexasaccharide*. The
833 Journal of biological chemistry, 1986. **261**(31): p. 14448-54.
- 834 44. Yates, E.A., et al., *1H and 13C NMR spectral assignments of the major sequences of twelve*
835 *systematically modified heparin derivatives*. Carbohydrate research, 1996. **294**: p. 15-27.
- 836 45. Byrne, D.P., et al., *cAMP-dependent protein kinase (PKA) complexes probed by*
837 *complementary differential scanning fluorimetry and ion mobility-mass spectrometry*. The
838 Biochemical journal, 2016. **473**(19): p. 3159-75.

- 839 46. Xu, R., et al., *Diversification of the structural determinants of fibroblast growth factor-heparin interactions: implications for binding specificity*. The Journal of biological chemistry, 2012. **287**(47): p. 40061-73.
- 840
- 841
- 842 47. Blackwell, L.J., et al., *High-throughput screening of the cyclic AMP-dependent protein kinase (PKA) using the caliper microfluidic platform*. Methods in molecular biology, 2009. **565**: p. 225-37.
- 843
- 844
- 845 48. Elkins, J.M., et al., *Comprehensive characterization of the Published Kinase Inhibitor Set*. Nature biotechnology, 2016. **34**(1): p. 95-103.
- 846
- 847 49. Jones, G., et al., *Development and validation of a genetic algorithm for flexible docking*. Journal of molecular biology, 1997. **267**(3): p. 727-48.
- 848
- 849 50. Korb, O., T. Stutzle, and T.E. Exner, *Empirical scoring functions for advanced protein-ligand docking with PLANTS*. Journal of chemical information and modeling, 2009. **49**(1): p. 84-96.
- 850
- 851 51. Huynh, M.B., et al., *Age-related changes in rat myocardium involve altered capacities of glycosaminoglycans to potentiate growth factor functions and heparan sulfate-altered sulfation*. The Journal of biological chemistry, 2012. **287**(14): p. 11363-73.
- 852
- 853
- 854 52. Dodson, C.A., et al., *A kinetic test characterizes kinase intramolecular and intermolecular autophosphorylation mechanisms*. Science signaling, 2013. **6**(282): p. ra54.
- 855
- 856 53. McSkimming, D.I., et al., *KinView: a visual comparative sequence analysis tool for integrated kinome research*. Molecular bioSystems, 2016. **12**(12): p. 3651-3665.
- 857
- 858 54. Caron, D., et al., *Mitotic phosphotyrosine network analysis reveals that tyrosine phosphorylation regulates Polo-like kinase 1 (PLK1)*. Science signaling, 2016. **9**(458): p. rs14.
- 859
- 860
- 861 55. Zhou, W., et al., *A fluorescence-based high-throughput assay to identify inhibitors of tyrosylprotein sulfotransferase activity*. Biochemical and biophysical research communications, 2017. **482**(4): p. 1207-1212.
- 862
- 863
- 864 56. Davies, S.P., et al., *Specificity and mechanism of action of some commonly used protein kinase inhibitors*. The Biochemical journal, 2000. **351**(Pt 1): p. 95-105.
- 865
- 866 57. Sun, C., et al., *HaloTag is an effective expression and solubilisation fusion partner for a range of fibroblast growth factors*. PeerJ, 2015. **3**: p. e1060.
- 867
- 868 58. Rudolf, A.F., et al., *A comparison of protein kinases inhibitor screening methods using both enzymatic activity and binding affinity determination*. PloS one, 2014. **9**(6): p. e98800.
- 869
- 870 59. Bailey, F.P., et al., *The Tribbles 2 (TRB2) pseudokinase binds to ATP and autophosphorylates in a metal-independent manner*. The Biochemical journal, 2015. **467**(1): p. 47-62.
- 871
- 872 60. Milani, M., et al., *DRP-1 is required for BH3 mimetic-mediated mitochondrial fragmentation and apoptosis*. Cell death & disease, 2017. **8**(1): p. e2552.
- 873
- 874 61. Hay, D.A., et al., *Discovery and optimization of small-molecule ligands for the CBP/p300 bromodomains*. Journal of the American Chemical Society, 2014. **136**(26): p. 9308-19.
- 875
- 876 62. Niehrs, C., et al., *Analysis of the substrate specificity of tyrosylprotein sulfotransferase using synthetic peptides*. The Journal of biological chemistry, 1990. **265**(15): p. 8525-32.
- 877
- 878 63. Lee, R.W. and W.B. Huttner, *(Glu62, Ala30, Tyr8)_n serves as high-affinity substrate for tyrosylprotein sulfotransferase: a Golgi enzyme*. Proceedings of the National Academy of Sciences of the United States of America, 1985. **82**(18): p. 6143-7.
- 879
- 880
- 881 64. Rudd, T.R. and E.A. Yates, *A highly efficient tree structure for the biosynthesis of heparan sulfate accounts for the commonly observed disaccharides and suggests a mechanism for domain synthesis*. Molecular bioSystems, 2012. **8**(5): p. 1499-506.
- 882
- 883
- 884 65. Yoshida-Moriguchi, T., et al., *SGK196 is a glycosylation-specific O-mannose kinase required for dystroglycan function*. Science, 2013. **341**(6148): p. 896-9.
- 885
- 886 66. Zhu, Q., et al., *Structure of protein O-mannose kinase reveals a unique active site architecture*. eLife, 2016. **5**.
- 887
- 888 67. McGeary, R.P., et al., *Suramin: clinical uses and structure-activity relationships*. Mini reviews in medicinal chemistry, 2008. **8**(13): p. 1384-94.
- 889
- 890 68. Givens, J.F. and K.F. Manly, *Inhibition of RNA-directed DNA polymerase by aurintricarboxylic acid*. Nucleic acids research, 1976. **3**(2): p. 405-18.
- 891
- 892 69. Gschwendt, M., et al., *Rottlerin, a novel protein kinase inhibitor*. Biochemical and biophysical research communications, 1994. **199**(1): p. 93-8.
- 893

- 894 70. Lackey, K., et al., *The discovery of potent cRaf1 kinase inhibitors*. Bioorganic & medicinal
895 chemistry letters, 2000. **10**(3): p. 223-6.
- 896 71. Xu, D., et al., *Engineering sulfotransferases to modify heparan sulfate*. Nature chemical
897 biology, 2008. **4**(3): p. 200-2.
- 898 72. Wu, Z.S., et al., *Suramin blocks interaction between human FGF1 and FGFR2 D2 domain
899 and reduces downstream signaling activity*. Biochemical and biophysical research
900 communications, 2016. **477**(4): p. 861-867.
- 901 73. Antolin, A.A., et al., *Objective, Quantitative, Data-Driven Assessment of Chemical Probes*.
902 Cell chemical biology, 2018. **25**(2): p. 194-205 e5.
- 903 74. Cohen, P., *Guidelines for the effective use of chemical inhibitors of protein function to
904 understand their roles in cell regulation*. The Biochemical journal, 2009. **425**(1): p. 53-4.

905

906

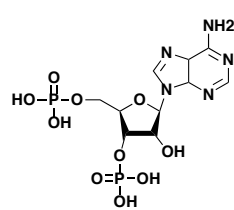
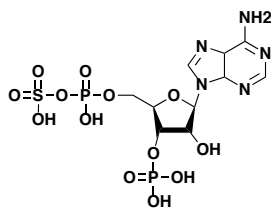
907

Figure 1

3'-phosphoadenosine-5'-phosphosulphate (PAPS)

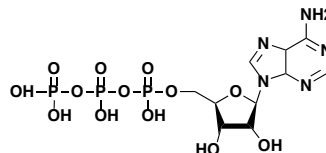
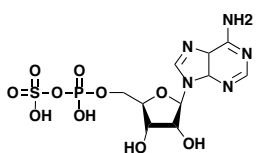
3'-phosphoadenosine-5'-phosphate (PAP)

A

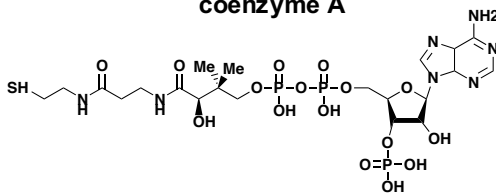


adenosine 5'-phosphosulphate (APS)

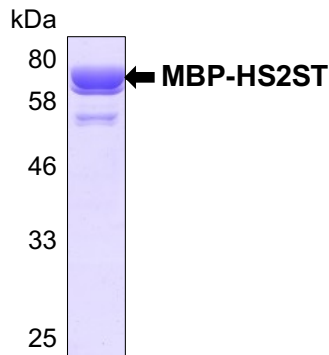
adenosine 5'-phosphate (ATP)



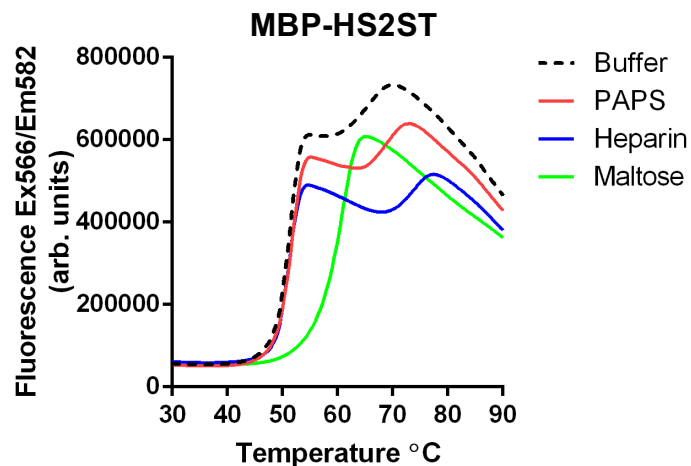
coenzyme A



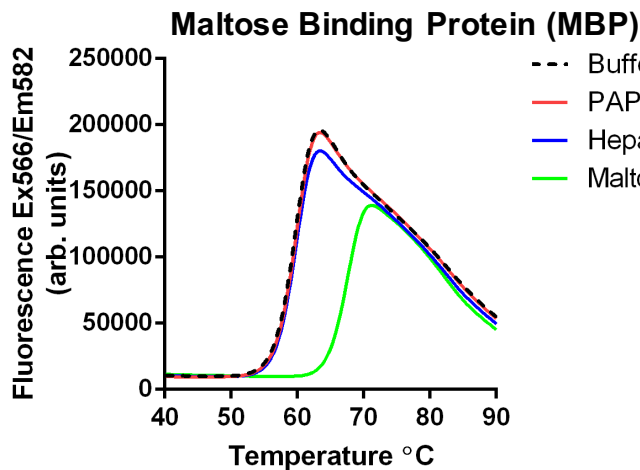
B



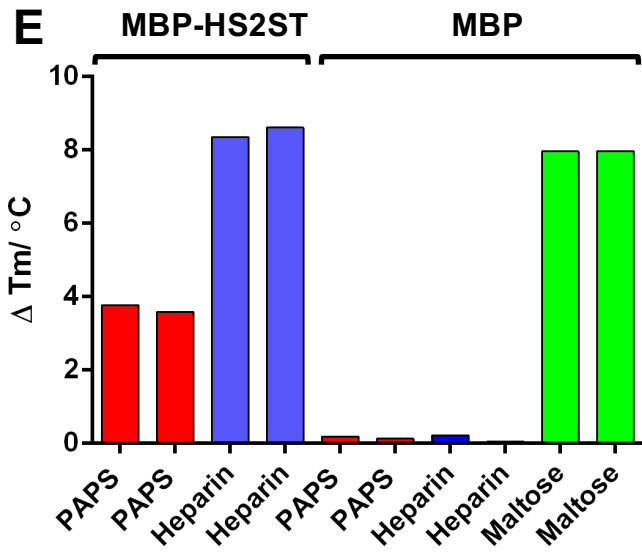
C



D



E



F

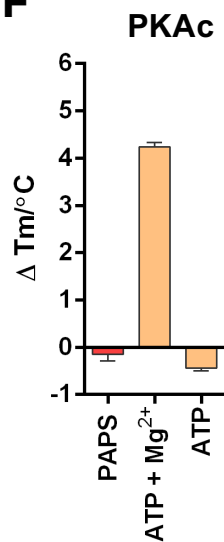


Figure 2

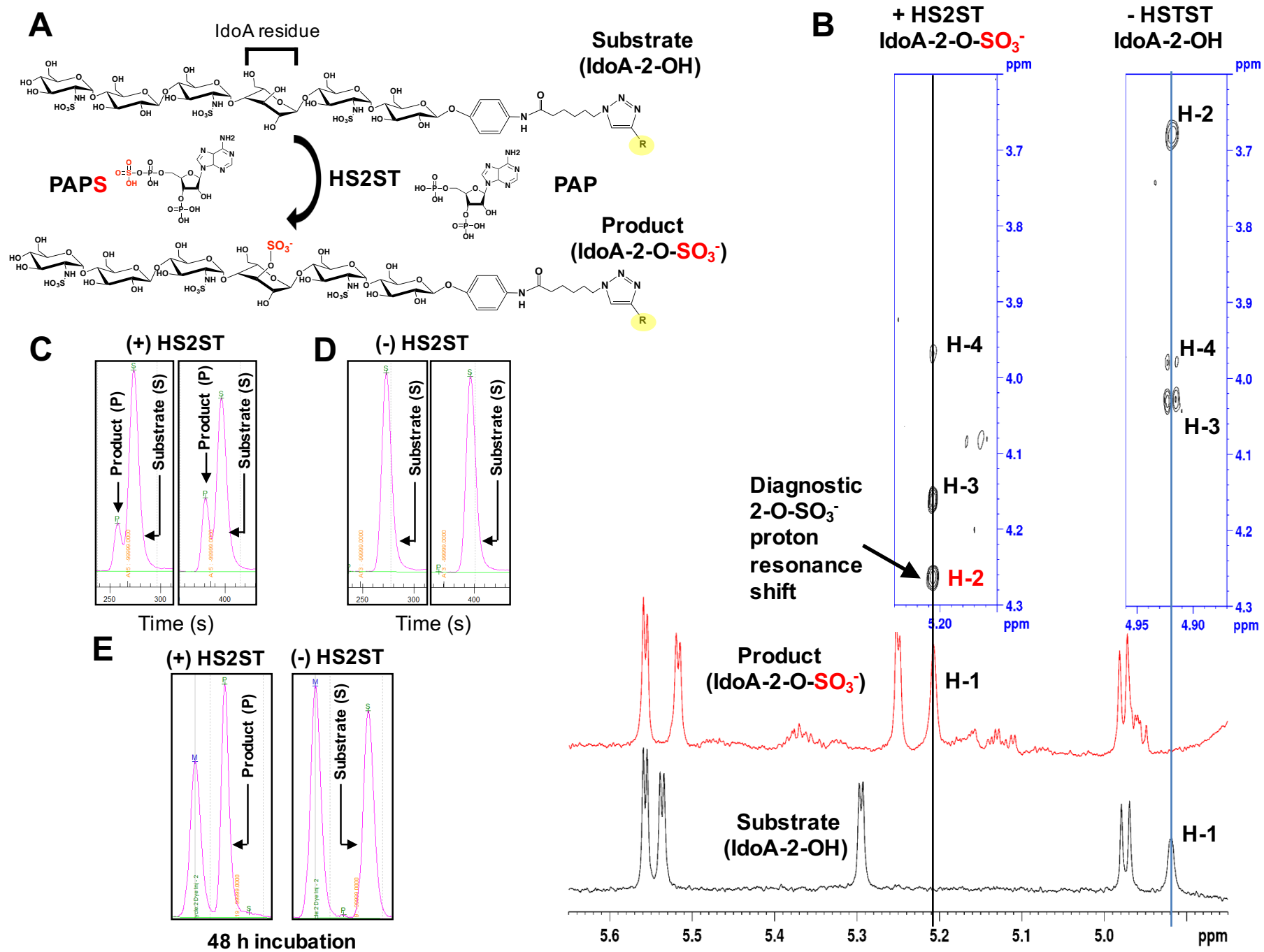


Figure 2 continued

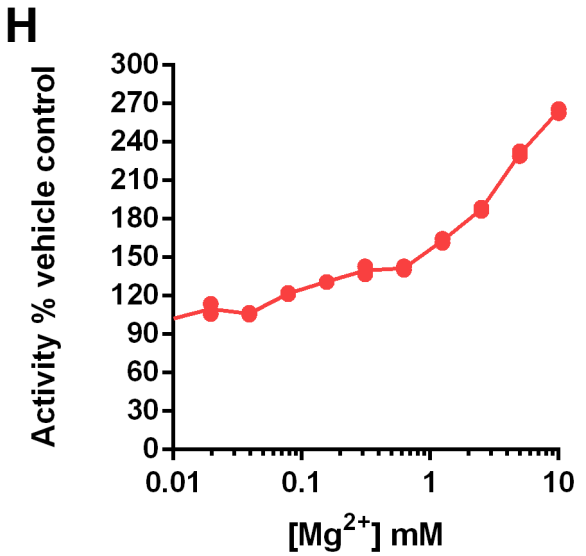
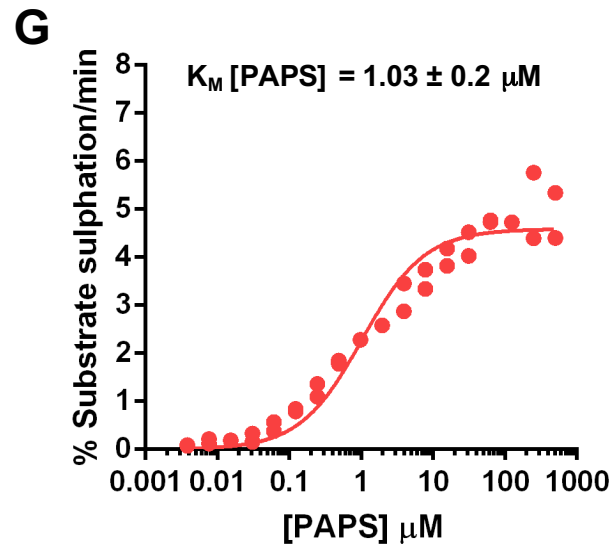
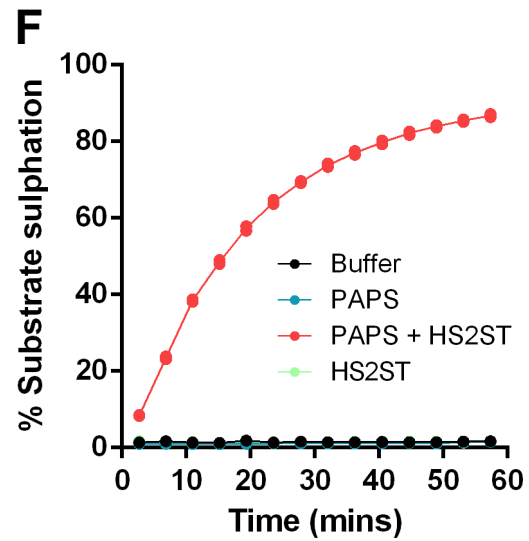


Figure 3

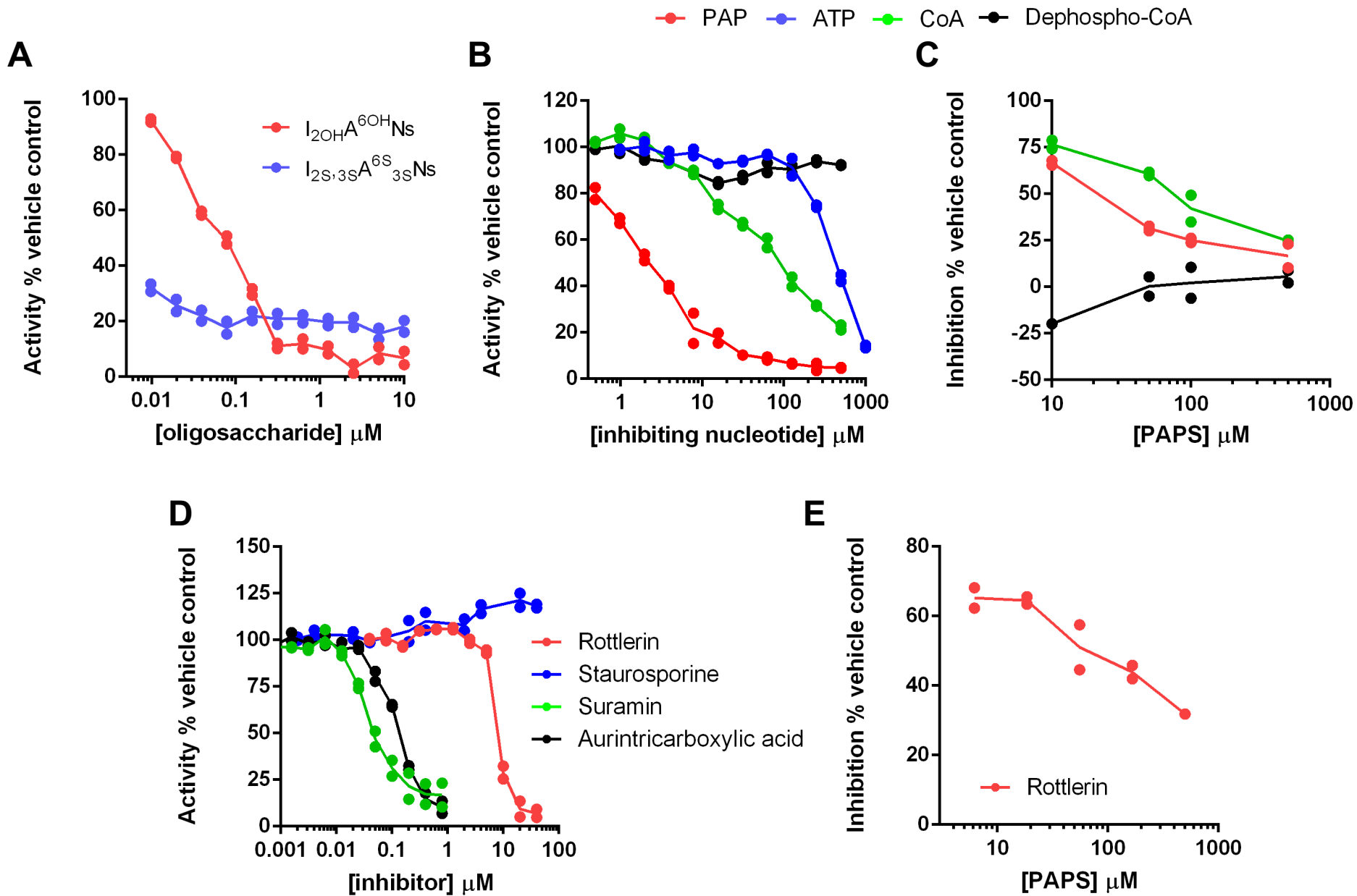
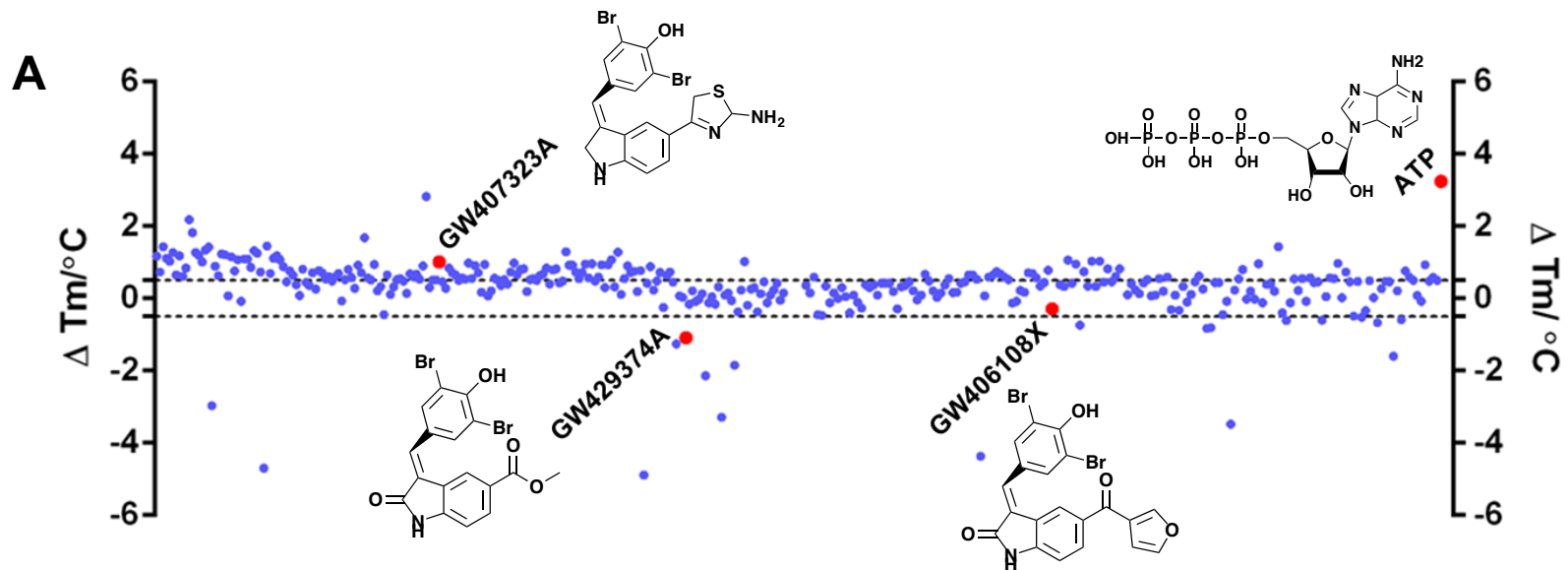
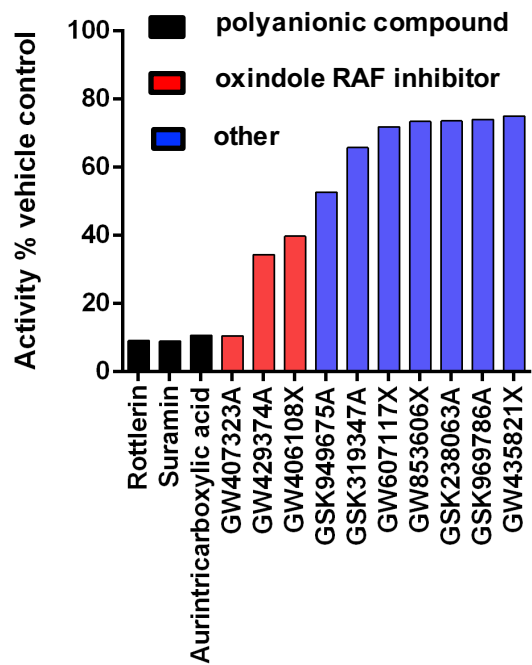


Figure 4



B



C

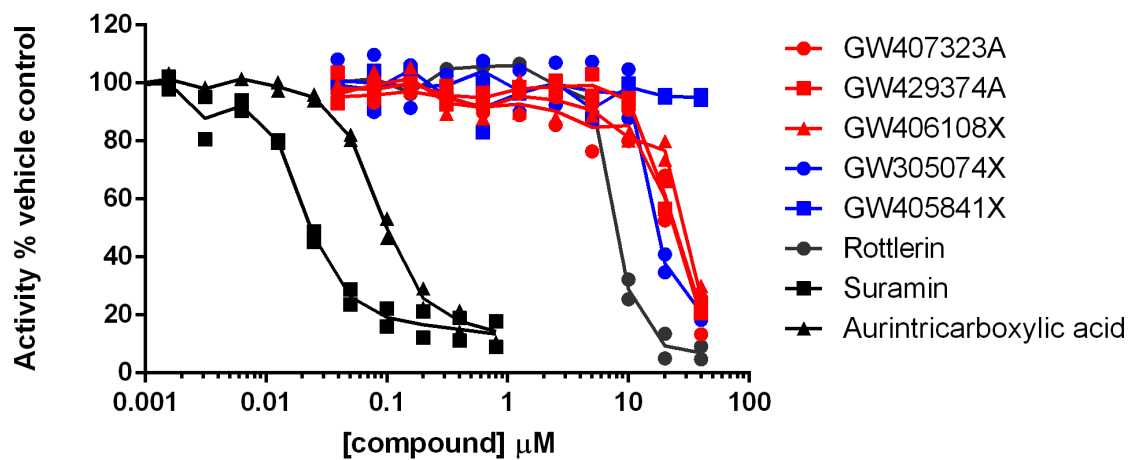
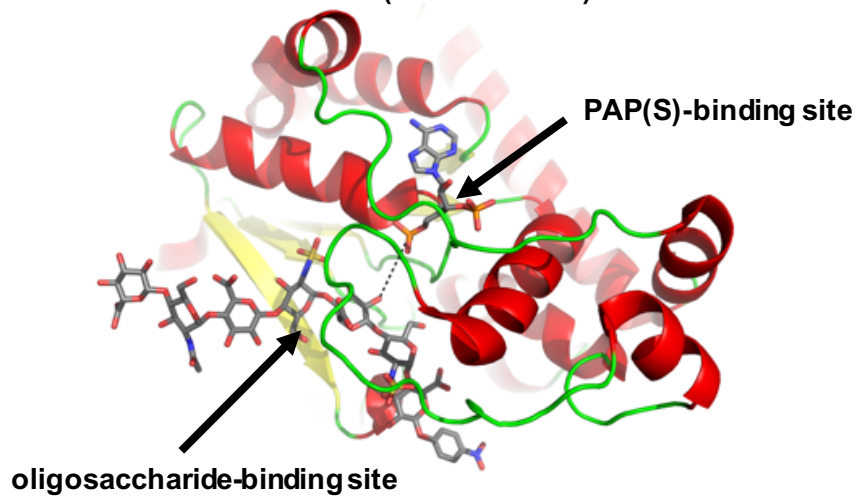


Figure 5

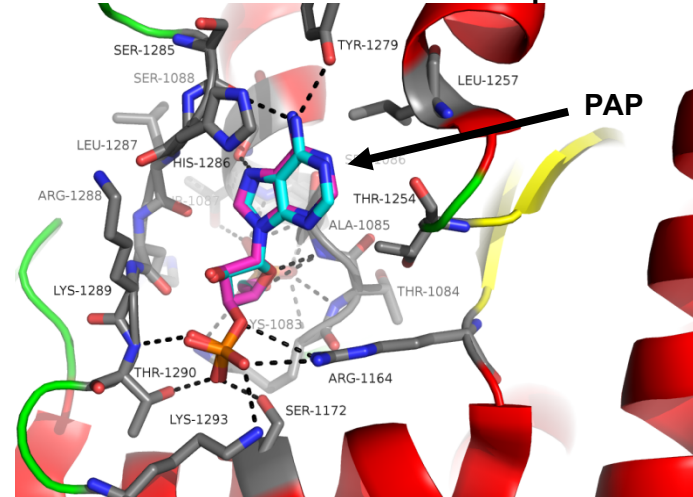
A

HS2ST active site (PDB ID: 4NDZ)



B

HS2ST:PAP complex



C

rottlerin

THR-1290

PAPS-binding site

D

GW407323A

ARG-1080

ASN-1112

Glycan-binding site

E

suramin

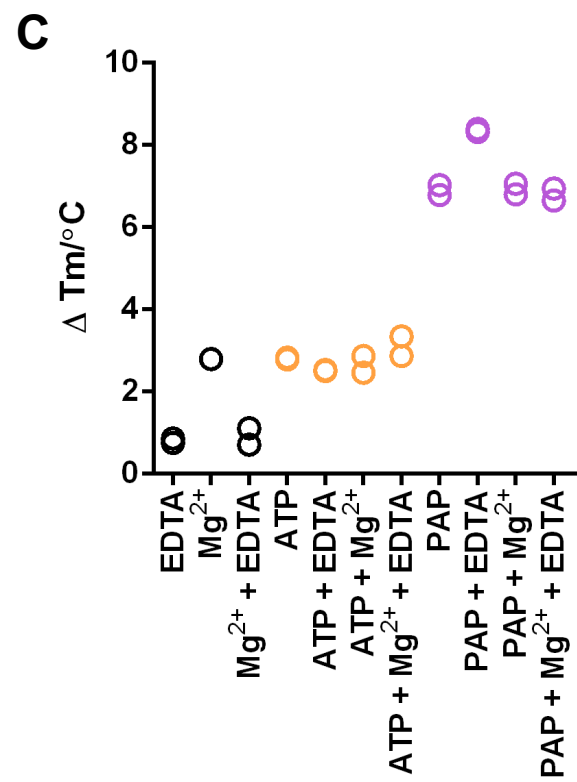
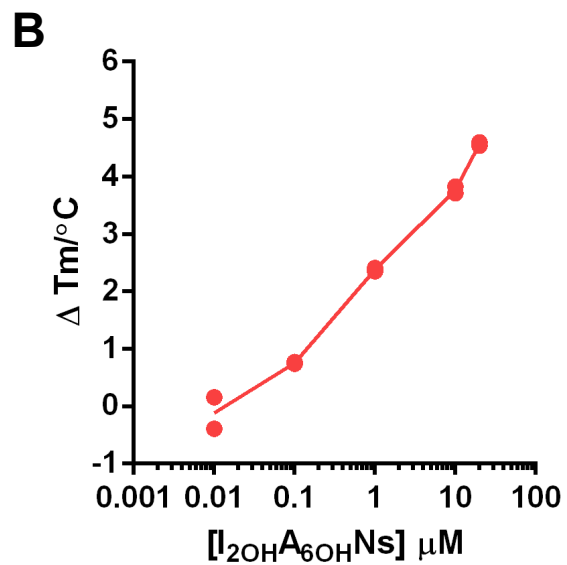
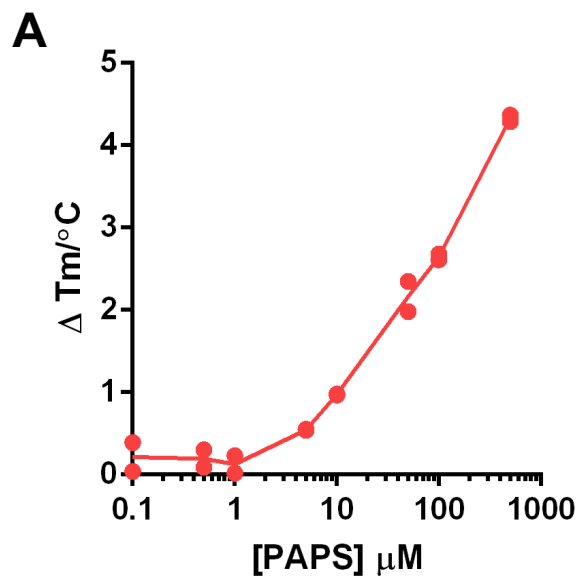
ASN-1091

ARG-1288

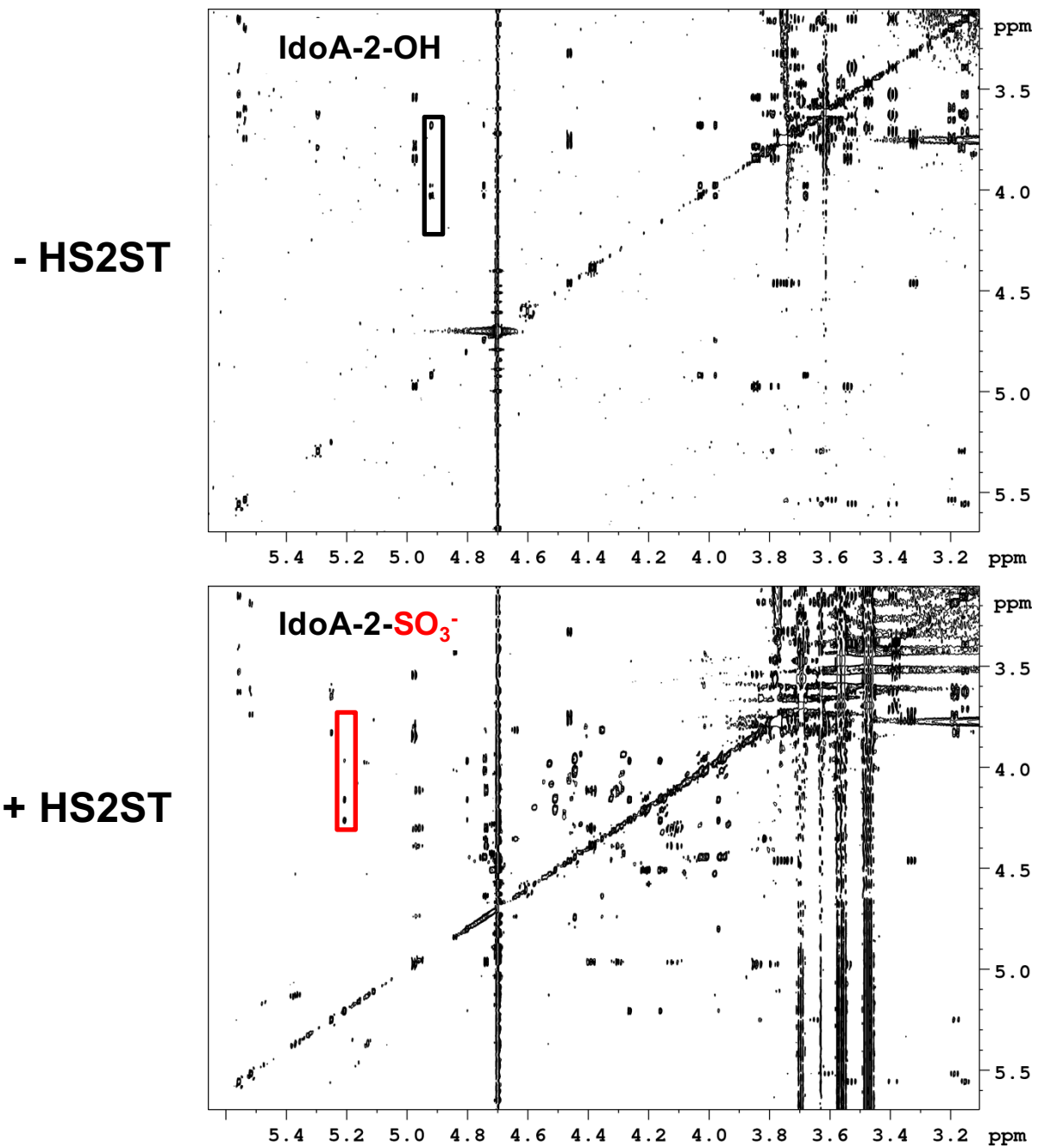
TYR-1094

Glycan and PAPS-binding sites

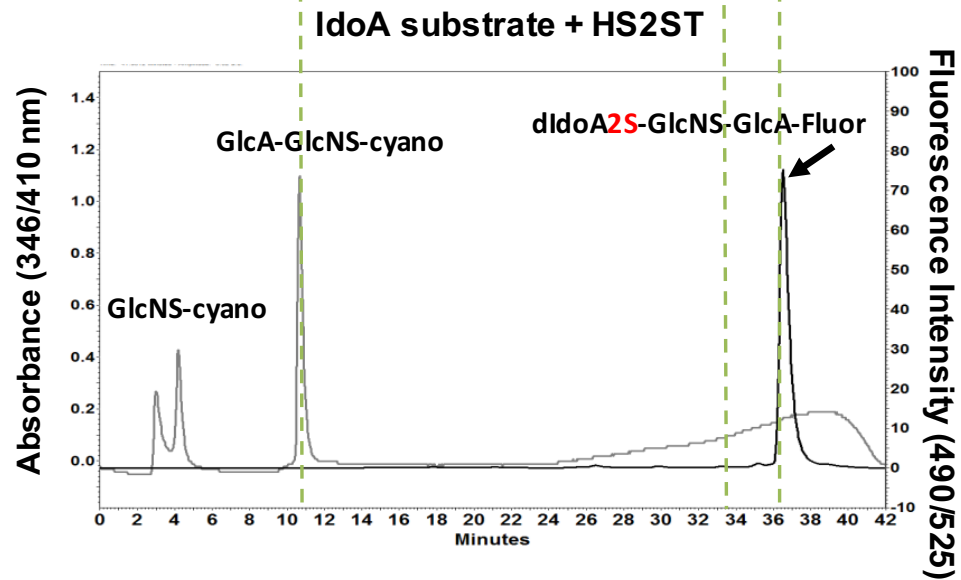
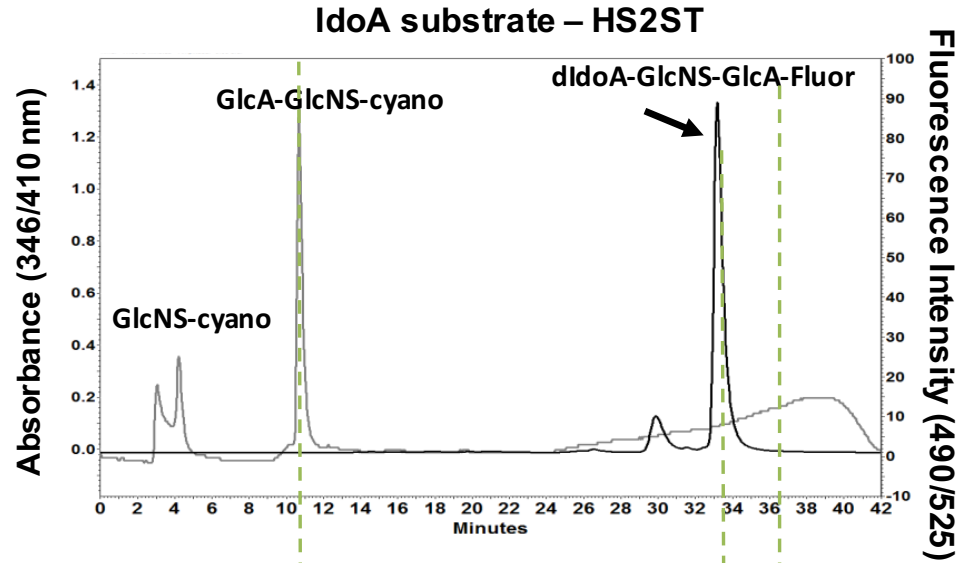
Supplementary Figure 1



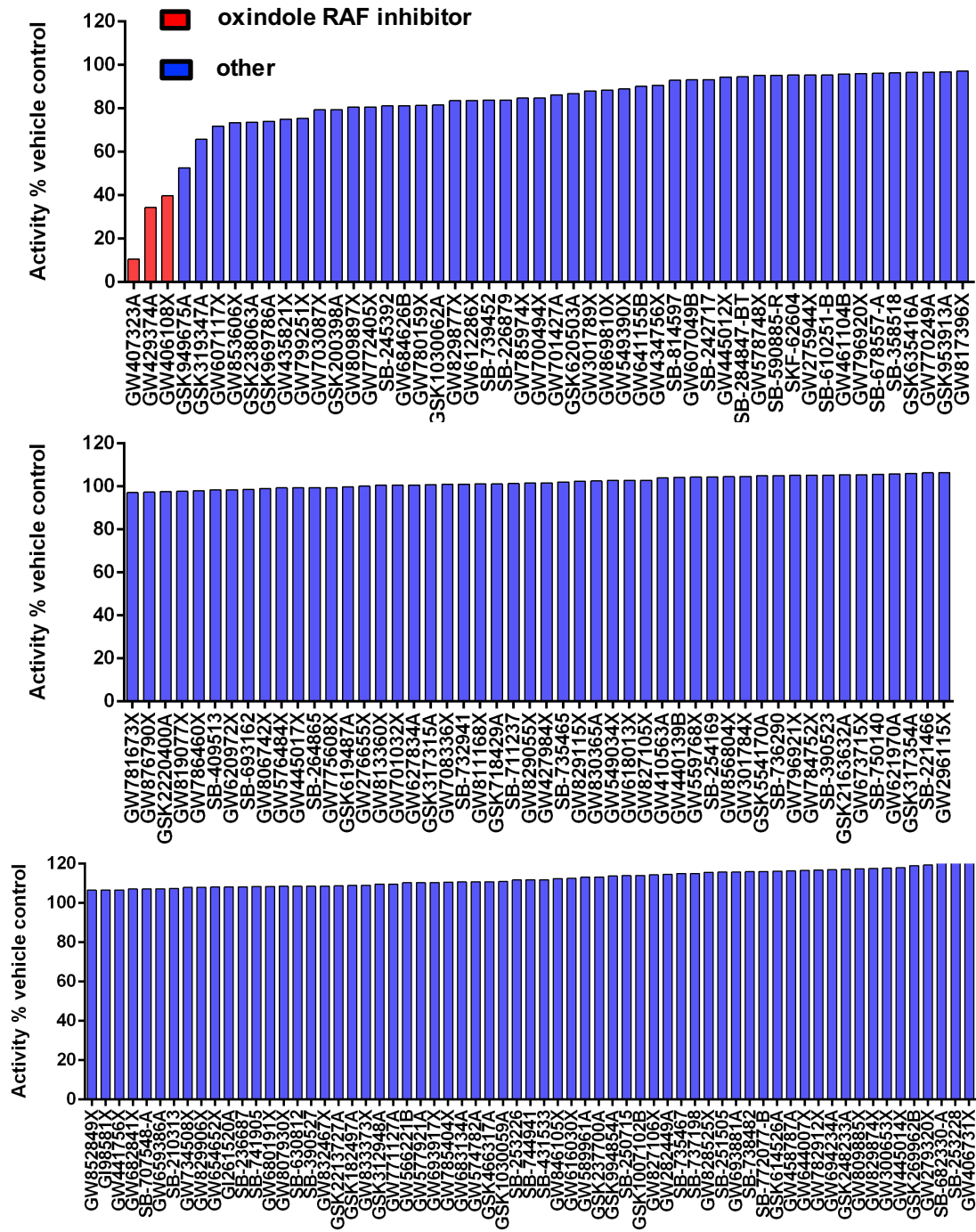
Supplementary Figure 3



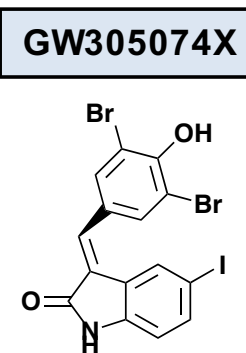
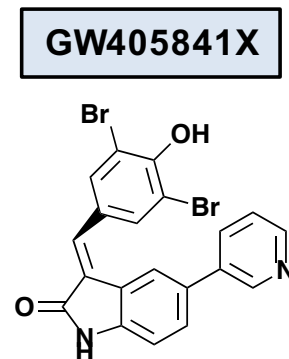
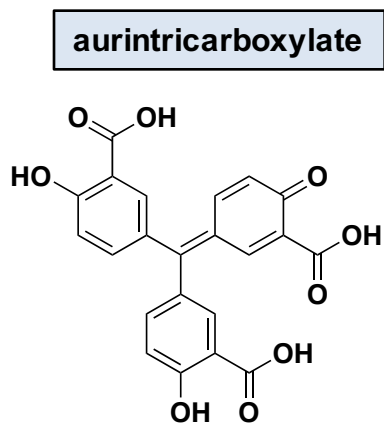
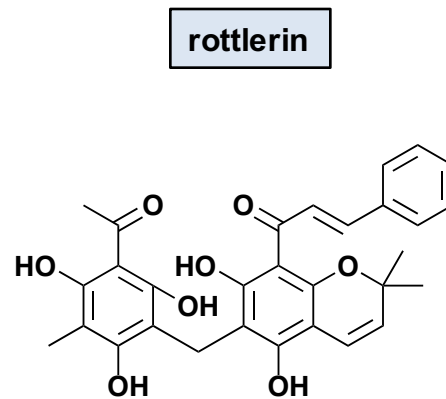
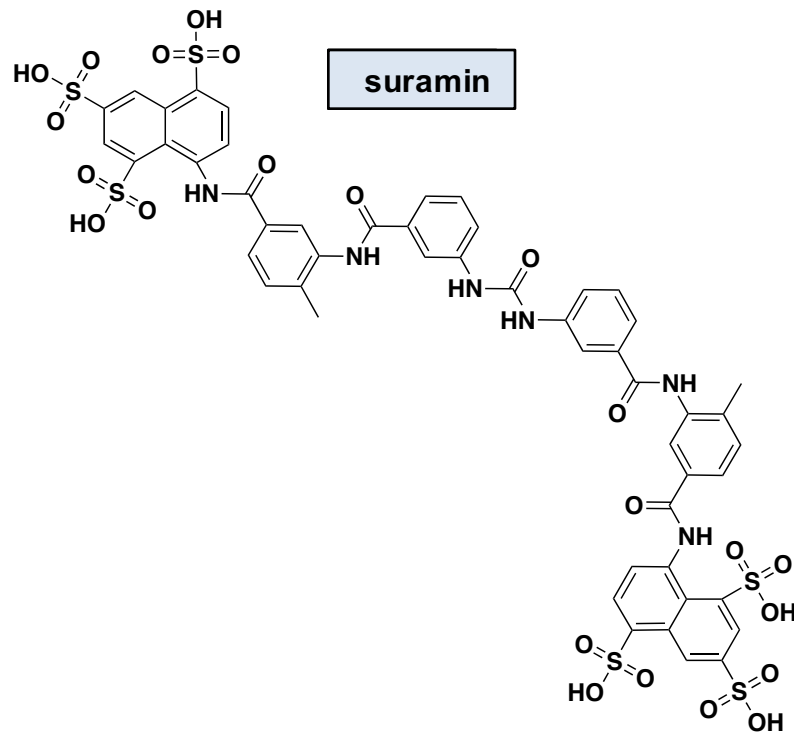
Supplementary Figure 4



Supplementary Figure 6



Supplementary Figure 7



Supplementary Figure 8

